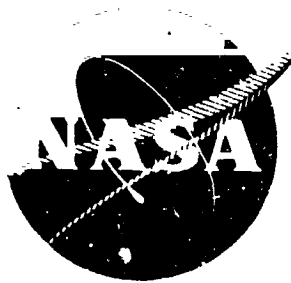


NASA CR-54217
WAED65. 12E



An Experimental Model of a 2KW, 2500 Volt Power Converter
for Ion Thrusters Using Silicon Transistors
in a Pulse-Width-Modulated Bridge Inverter

by

G. W. Ernsberger

prepared for

NATIONAL AERONAUTICS AND SPACE ADMINISTRATION

Contract NAS3-5918

PRICE \$ _____

PRICE(S) \$ _____

Hard copy (HC) \$3.00

Microfiche (MF) .75



WESTINGHOUSE ELECTRIC CORPORATION
AEROSPACE ELECTRICAL DIVISION
LIMA, OHIO

N 65-21432

(ACCESSION NUMBER)

(PAGES)

CB-54217

(NASA CR OR TMX OR AD NUMBER)

(THRU)

(CODE)

03

(CATEGORY)

SUMMARY REPORT

An Experimental Model of a 2KW, 2500 Volt Power Converter
for Ion Thrustors Using Silicon Transistors
in a Pulse-Width-Modulated Bridge Inverter

by

G. W. Ernsberger

prepared for

NATIONAL AERONAUTICS AND SPACE ADMINISTRATION

March 1, 1965

Contract NAS3-5918

Technical Management
NASA Lewis Research Center
Cleveland, Ohio
Spacecraft Technology Division
Bernard L. Sater

WESTINGHOUSE ELECTRIC CORPORATION
AEROSPACE ELECTRICAL DIVISION
Box 989,
Lima, Ohio 45801

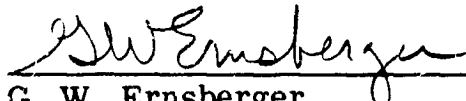
(UNCLASSIFIED)

NASA CR-54217
Report No. WAED65.12E


March 1, 1965


An Experimental Model of a 2KW, 2500 Volt Power Converter
for Ion Thrusters Using Silicon Transistors
in a Pulse-Width-Modulated Bridge Inverter


Prepared by:


G. W. Ernsberger
Conversion Systems Engineering

Approved by:


H. B. James
Supvr. Advanced Program Engineering
Section


H. B. Saldin
Mgr. Advanced Program Engineering
Section


N. W. Bucci
Mgr. Engineering Department

(UNCLASSIFIED)

PREFACE

The author wishes to acknowledge the technical assistance of Messrs. T. M. Heinrich, A. Kernick, D. M. Lamaster, W. E. Hawley, J. W. Ogden, H. R. Howell, and C. R. Merola, all of Westinghouse Electric Corporation, Lima, Ohio. The author also wishes to acknowledge the technical guidance and direction of Messrs. R. L. Gasperetti and H. B. James of Westinghouse Electric Corporation and Bernard L. Sater and V. Lalli of the NASA Lewis Research Center.

An Experimental Model of a 2KW, 2500 Volt Power Converter
for Ion Thrustors Using Silicon Transistors
in a Pulse-Width-Modulated Bridge Inverter

by

G. W. Ernsberger

ABSTRACT

21432
This report covers the work carried out under Phase I of Contract NAS3-5918. Two power supply models were built and evaluated. The test program demonstrated that using silicon power transistors in a pulse width modulated bridge inverter with current feedback base drive is an effective and desirable method of building a reliable, lightweight and efficient power converter for ion thrustors.

H. H. H.

TABLE OF CONTENTS

SECTION		PAGE
	PREFACE	i
	ABSTRACT	ii
	LIST OF ILLUSTRATIONS	v
	LIST OF TABLES	viii
	SUMMARY	ix
I	INTRODUCTION	1
II	CONVERTER DESIGN CONSIDERATIONS	2
	A. SILICON POWER TRANSISTOR SELECTION .	2
	B. INVERTER FREQUENCY SELECTION	2
	C. CIRCUIT DESIGN	5
III	BREADBOARD MODEL EVALUATION	9
	A. PERFORMANCE OF CONTROL AND PRO- TECTION FUNCTIONS	9
	B. STATIC LOAD TESTS	10
	C. COMPONENT ELECTRICAL STRESS TESTS .	13
	D. COMPONENT FAILURES AND CORREC- TIVE ACTION	16
IV	POWER TRANSISTOR EVALUATION	18
	A. CURRENT GAIN	18
	B. BASE-TO-EMITTER FORWARD DROP	20
	C. SATURATION RESISTANCE	20
	D. SWITCHING SPEED	20
	E. LOSSES	23
V	EXPERIMENTAL MODEL EVALUATION	28
	A. PRELIMINARY CHECKOUT OF EXPERI- MENTAL MODEL AND DESIGN IMPROVEMENTS	28
	B. STATIC LOAD TESTS	30
	C. COMPONENT ELECTRICAL STRESS TESTS .	38
	D. ENDURANCE TESTS	46

TABLE OF CONTENTS (Cont.)

SECTION		PAGE
VI	WEIGHT, LOSS, AND PERFORMANCE CONSIDERATIONS.....	51
VII	CONCLUSIONS AND RECOMMENDATIONS	55
APPENDIX A.	PARTS LIST FOR EXPERIMENTAL MODEL.	57

LIST OF ILLUSTRATIONS

FIGURE	TITLE	PAGE
1	Calculated Effect of Inverter Frequency on Power System Weight	4
2	Schematic Diagram of 2KW, 2500 Volt Power Converter for Ion Thrusters	6
3	Voltage Regulation Curves for 2KW, 2500 D. C. Power Converter Breadboard Model	11
4	Efficiency Versus Load for 2KW, 2500 D. C. Power Converter Breadboard Model	12
5	Output Voltage Ripple	14
3	Application and Removal of a Short Circuit. (60 MS duration) with the Overcurrent Trip Circuit Disconnected	15
7	Common-Emitter Collector Characteristics of STC-2118.....	19
8	Base-Emitter Characteristics of STC-2118.....	19
9	Transistor Turn-On Transient with 36 Ampere Load in Figure 11 Test Circuit	21
10	Transistor Turn-Off Transient with 26 Ampere Load in Figure 11 Test Circuit	21
11	Test Circuit for Measuring Transistor STC 2118 Switching Speed	22
12	Transistor Turn-On Transient in Power Supply with 30 Ampere Collector Current Shown in Figure 14	24
13	Transistor Turn-Off Transient in Power Supply with 22 Ampere Collector Current Shown in Figure 14	24
14	Transistor Collector Current with 1 PU Load on the Power Supply (T & M Research Products Shunt Type F-500-2)	25

LIST OF ILLUSTRATIONS (Cont.)

FIGURE	TITLE	PAGE
15	Calibration of Transistor Heat Sink	26
16	Rear View of Experimental Model	29
17	Laboratory Setup for Static Load and Electrical Stress Tests	31
18	Soft-On Time Constant Range with 22 MFD Capacitor C12	33
19	Soft-On Time Constant Range with 1 MFD Capacitor C12A	34
20	Experimental Model Output Voltage Plotted as a Function of Load	35
21	Experimental Model Efficiency Plotted as a Function of Load	36
22	Input Current Ripple with Full-Load and No-Load on the Experimental Model	37
23	Calibration Oscillogram Showing Normal Full-Load Operation	42
24	Oscillogram Showing Application of Short Circuit with Maximum Overcurrent and Blink-Off Time Delays	43
25	Oscillogram Showing Application of Short Circuit with Minimum Overcurrent and Blink-Off Time Delays	44
26	Oscillogram Showing Removal of Short Circuit with Vacuum Relay	45
27	Oscillogram Showing Application of Short Circuit with a Vacuum Relay	47
28	Oscillogram Showing Shut-Down of Power Converter with Low Level Control Signal	48

LIST OF ILLUSTRATIONS (Cont.)

FIGURE	TITLE	PAGE
29	Oscillogram Showing Application and Removal of Short Circuit	49

LIST OF TABLES

NUMBER	TITLE	PAGE
I	Calculated Weights and Losses of Components Which Are Affected by Frequency.....	3
II	Component Safety Factors with Rated Load	39
III	Component Safety Factors with Hydrogen Thyratron and Vacuum Relay Transient Breakdown Devices	40
IV	Component Weight Analysis	52
V	Component Loss Analysis	53

An Experimental Model of a 2KW, 2500 Volt Power Converter
for Ion Thrusters Using Silicon Transistors
in a Pulse-Width-Modulated Bridge Inverter

by

G. W. Ernsberger

Westinghouse Electric Corporation

SUMMARY

This report covers the work carried out under Phase I of Contract NAS3-5918. The object of this program was to design, fabricate, and test a power converter for ion thrusters employing a pulse width modulated bridge inverter with silicon power transistors using current feedback base drive. The goals were to develop a reliable, efficient and lightweight power supply which would minimize the complete space power system weight. This contract required that a Breadboard Model and an Experimental Model be tested with static and transient loads to verify feasibility and merits.

All contract objectives have been fulfilled. A 2KW Experimental Model has been delivered which has a full load efficiency of 87.8% and a total component weight of 28.2 pounds. This model, during an evaluation program, supplied current to over 400 short circuit transients, blinked-off and automatically re-applied output voltage or current in a soft-on manner over 100,000 times, and operated at full load for over 10 hours without component failures. Analysis shows that this component weight could be reduced to approximately 11.3 pounds by eliminating the input current ripple limits, by eliminating the variable output overcurrent time delay requirements, and by reducing the efficiency to approximately 85%.

I. INTRODUCTION

The majority of ion thruster development work has been done with laboratory type power supplies. Compared to engine development, only a small amount of effort has been expended on the development of highly efficient, lightweight, and reliable power supplies for use with ion thrusters. In addition, no power supply has been available with variable operating characteristics which would allow engine arcing and its effects to be minimized.

The purpose of this development effort has been to design, develop, build and test an Experimental Model of a 2KW 2500 volt power converter for ion thrusters, and to demonstrate the feasibility of advanced concepts and techniques for obtaining improvements in weight, reliability and efficiency of these devices. In accordance with contract requirements, this power converter uses current feedback to drive silicon power transistors in a pulse-width-modulated bridge inverter. Upon application of a short circuit to the power converter output terminals, the converter will automatically:

1. Supply approximately 1.25 PU current to the fault for a manually adjustable period of time (overcurrent time delay 2 to 18 ms),
2. Turn itself off for a manually adjustable period of time (blink-off time delay 2 to 50 ms), and
3. Turn itself on and reapply output voltage at a manually adjustable rate (soft-on from 2 to 2000 ms).

If the fault has not cleared, this cycle of events will repeat indefinitely until a low level control signal is used to turn the converter off. These automatic controls and variable operating characteristics are intended to eliminate the damaging effects of arcing on the power converter and to enable the power converter operating characteristics to be matched with those supply characteristics which are best suited to the ion thruster. Operation of the power converter with an electron bombardment ion thruster is not part of this contract.

A similar Experimental Model is being developed on Contract NAS3-5917. This similar converter has identical electrical requirements and ratings but uses gate controlled switches (GCS) rather than transistors for the power switching elements, and is regulated by phase shifting one GCS inverter relative to a second GCS inverter. The results of these two contracts and subsequent operation of both power converters with an ion thruster will provide a good comparison of the feasibility and merits of these two types of power switching devices and regulation methods.

This summary report covers the results of the entire seven month program which was initiated June 30, 1964.

II. CONVERTER DESIGN CONSIDERATIONS

A. SILICON POWER TRANSISTOR SELECTION

The first design consideration was the selection of the silicon power transistors. For minimum converter weight and high efficiency, it is desirable to use a fast switching transistor at a reasonably high frequency. Also, the transistor current and voltage ratings should be high enough so that four transistors in a bridge circuit can provide a 2KW output with a safety factor of 2 on the V_{CE} and collector current ratings.

The best available transistor for this application is the Silicon Transistor Corporation Type 2118. This transistor has a maximum collector current rating of 65 amperes and a maximum collector-to-emitter voltage rating of 200 volts. Rated minimum d-c gain of the transistor is 10 at 50 amperes collector current. The saturation resistance is rated at 0.03 ohms maximum with 50 amperes collector current. The published maximum switching times are $t_r = 15$ microseconds and $t_f = 9$ microseconds.

It was a contract design objective to maintain a minimum safety factor of two on both current and voltage ratings and a minimum safety factor of four in allowable dissipation for semiconductors. This objective established the bridge inverter input voltage at 100 volts d-c since each transistor in a bridge inverter is required to withstand the total input voltage.

B. INVERTER FREQUENCY SELECTION

The inverter operating frequency of 800 cps was selected to obtain a minimum power system weight. To make this frequency selection, it was necessary to calculate the effect of frequency on the power converter component weights and losses. The weights and losses of components which are affected by frequency were calculated for operating frequencies of 400, 800, and 1200 cps. A summary of these weight and loss calculations is given in Table I.

The calculated magnetic component weights include the weight of insulation and mounting brackets which are relatively unaffected by frequency. The power transistor losses listed in the table are switching losses based on the maximum switching times given above. The base drive, conduction, and leakage transistor losses are not included in the table because they are not appreciably affected by frequency.

TABLE I. Calculated Weights and Losses of Components
Which Are Affected by Frequency

Component	400 cps		800 cps		1200 cps	
	Loss (Watts)	Weight (Pounds)	Loss (Watts)	Weight (Pounds)	Loss (Watts)	Weight (Pounds)
Input Choke (L1)	NA	1.3	NA	0.65	NA	0.43
Input Capacitor (C1)	0.5	1.1	1.0	0.55	1.5	0.37
Power Transistors (Q1-4)	44	NA	88	NA	132	NA
Output Transformer (T1)	60	6	49	4.4	44	3.8
Output Choke (L2)	NA	18	NA	9	NA	6
Output Capacitor (C2)	NA	4.3	NA	2.1	NA	1.4
Totals	104.5	30.7	138	16.7	177.5	12.0
NA = not affected or negligible change						

The losses of the components given in Table I must, in a complete system, be supplied by a silicon solar cell array and eventually be radiated to space by a waste heat radiator. According to the contract scope of work, present silicon solar cell arrays have specific weights of approximately 200 pounds per kilowatt. It was estimated that a waste heat radiator, operating at 125°C, would weigh 65 pounds per kilowatt. Using the conversion factor 0.265 pounds of solar cells and radiator per watt of loss, the frequency dependent losses in Table I were converted to pounds and plotted in Figure 1. The composite weight curve of Figure 1 was used to select 800 cps for the inverter operating frequency.

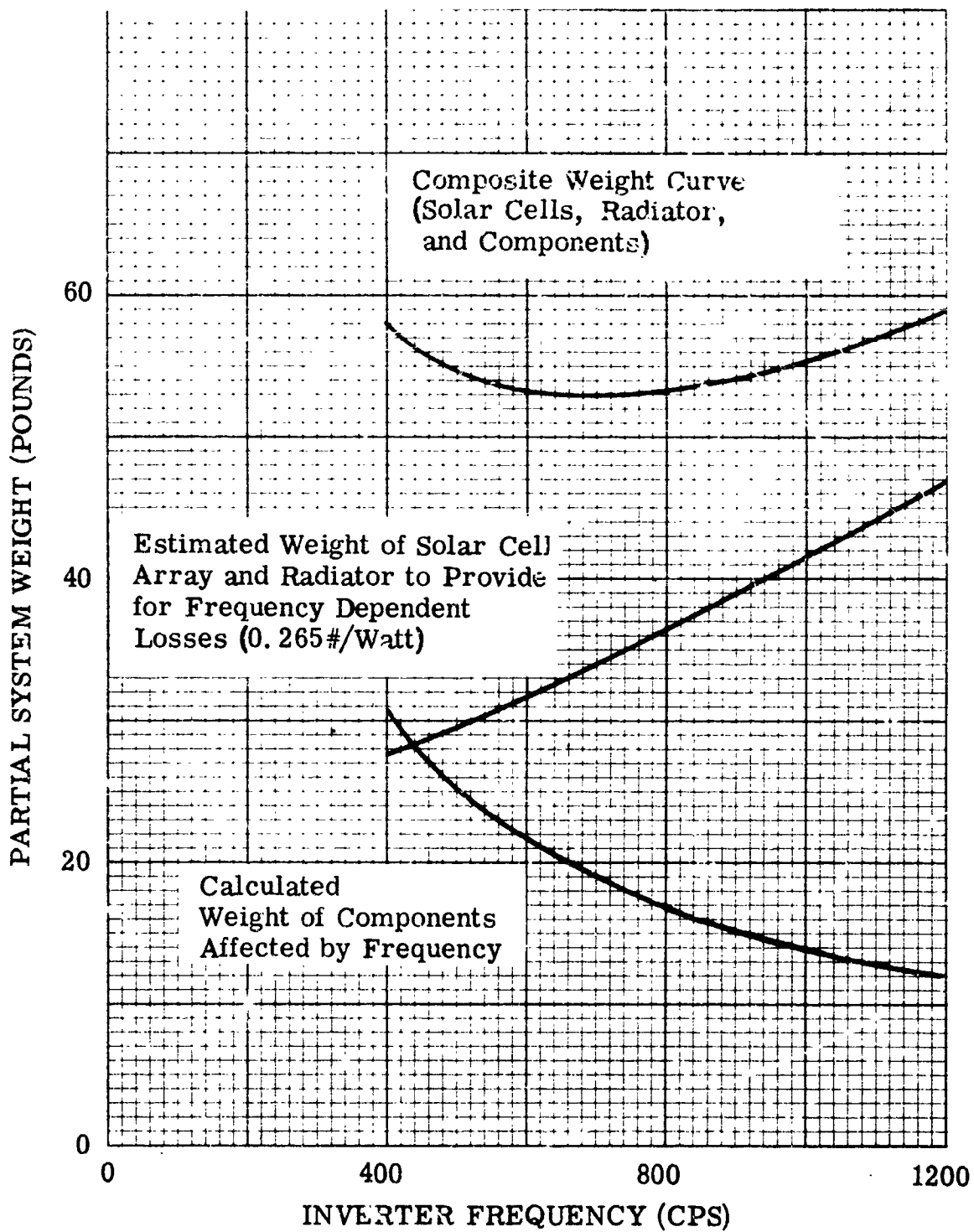


FIGURE 1. Calculated Effect of Inverter Frequency
on Power System Weight

WAED65. 12E-4

C. CIRCUIT DESIGN

The complete converter circuit which resulted from the design development, and evaluation of both the Breadboard and Experimental Models is shown schematically in Figure 2. A description of the electrical components is given in Appendix A.

1. Bridge Inverter Circuit

The converter circuit was designed around the basic bridge inverter which consists primarily of four silicon power transistors (Q1-Q4) and output transformer (T1). Base current for the power transistors is supplied by controlled current feedback transformers (T2-T5) and is directly proportional to collector current. The operation of the current transformers is controlled by transistors Q5-Q10. The input filter (L1 & C1) is used to limit the input current ripple in accordance with the contract scope of work.

2. Output Rectifier and Filter

A bridge rectifier (CR1-CR4) is used to rectify the pulse width modulated inverter output voltage. The output filter (L2 & C2) is required to meet the 5% limit on output ripple voltage. Resistors (R90-R97) in series with the output capacitor were added during the Breadboard Model evaluation to limit the peak capacitor current to 3 PU during periods of load breakdown. A transducer (AR1) senses the magnitude of output current and provides an input to the overcurrent sensing circuit (CR27-CR30, R60, Z6, Z11, and C11).

The output filter constants (3.9 Henry and 0.75 mfd) were determined by the necessity of limiting to 100% the increase in power transistor current during the first inverter cycle after a short circuit has been applied. This current delay prevents power transistor damage during the half-cycle period when the pulse width modulator circuit is responding to the overcurrent condition.

3. Pulse Width Modulator

Output voltage is regulated at 2500 volts d-c and output current is limited to approximately 1.25 PU by the pulse width modulator circuit. A regulated d-c voltage of approximately 19 volts is supplied to this and all control circuits by a d-c shopper circuit (Q23, Q33, Q37, and T12), series regulator transistor (Q11), and zener diode (Z5). This regulated voltage is applied to a Jensen type master oscillator (Q12, Q13, T9 and T11), which establishes the inverter operating frequency at 800 cps. This transformer (T9) drives two transistors (Q6 and Q7) which control the operation of half of the bridge inverter (Q1 and Q3).

The operation of the other half of the bridge inverter (Q2 and Q4) is phase delayed a controlled amount from 0° to 180° by a Ramey type magnetic amplifier (AR2 and AR3) and a flip-flop (Q14, Q15 and T10) which drives transistors Q9 and Q10. The Ramey type magnetic amplifier was chosen to control the inverter output pulse width because of its simplicity and fast half-cycle response. The amount of phase delay acting upon each half cycle by saturable reactors AR2 and AR3 is determined entirely by the volt-seconds available for flux reset during the previous half cycle. These volt-seconds are controlled by an emitter follower (Q27) which is controlled by the overcurrent sensing circuit, the output voltage sensing circuit (AR4), and the soft-on circuit.

4. Soft-On Circuit

The rate of rise of output voltage is controlled by the discharging rate of capacitor C12. The required adjustable time delay range of 2 to 2000 milliseconds is provided by selecting one of two time delay capacitors with switch SW2 and by adjusting the discharging resistance with variable resistor R55. The discharging capacitor voltage is transferred to the emitter follower in the pulse width modulator circuit (Q27) through transistor Q28 and diode CR21. Capacitor C12 can be charged to a fixed voltage level during the minimum blink-off period of two milliseconds through transistor Q25, resistor R53, and diode CR34.

5. Start-Up Time Delay

When input voltage is first applied to the power supply, a fixed time delay of approximately 27 milliseconds is provided by resistor R33, capacitor C8, and zener diode Z8 before base drive is applied to the silicon power transistors in the bridge inverter. This start-up time delay is provided to allow the Jensen oscillator to reach normal operating frequency and to allow the pulse width modulator to prepare for soft-on operation. At the end of the start-up time delay, the start bus is grounded through transistor Q19. This provides a path for emitter current from all four drive transistors Q6, Q7, Q9, and Q10.

6. Blink-Off and Overcurrent Time Delays

As required by the contract scope of work, the inverter will automatically turn off for an adjustable period of time (approximately 2 to 50 milliseconds) at the end of an adjustable overcurrent time delay. The blink-off period is initiated by an output voltage from the overcurrent time delay (R45, R46, C10, and Z10) which causes the silicon controlled rectifier (CR25) to conduct and turn off the start bus transistor (Q19). This turn-off is synchronized by transistor Q35 so that it occurs at the beginning of an output voltage cycle when both inverter transistors Q1

and Q3 have already been pulsed off by transistor Q5. The blink-off time delay is provided by adjustable resistor R39, resistor R40, capacitor C9, and unijunction transistor Q20. The blink-off time delay is ended by C9 discharging through R38 which momentarily turns transistor Q22 on and CR25 off. If an overcurrent condition no longer exists, then CR25 remains off, start bus transistor Q19 turns on, and the power supply returns soft-on.

III. BREADBOARD MODEL EVALUATION

The Breadboard Model of the power supply was evaluated with resistive load and was subjected to application and removal of short circuits using a knife switch as the shorting device. Several important features of the final design resulted from the breadboard evaluation and will be discussed in this section. The results of the Breadboard Model testing will be presented in this section in four separate categories: performance of control and protection functions; static load tests; component electrical stress tests; and component failures and corrective action.

A. PERFORMANCE OF CONTROL AND PROTECTION FUNCTIONS

1. Start-Up Time Delay

With the on-off switch in the "on" position when power was applied to the input terminals of the unit, there was a 27 millisecond delay before the power supply came soft-on. This time delay is not affected by blink-off and does not operate again until power is removed and then re-applied to the input terminals.

2. Soft-On Time Delay

The soft-on time delay controls the rate-of-rise of the output voltage on initial start-up and when the unit returns on after blinking-off. The soft-on time delay was adjustable from 1.6 milliseconds to 6 seconds by using two capacitors that are selected by means of a toggle switch. The time delay was adjustable from 1.6 to 160 milliseconds with one capacitor and was adjustable from 0.060 to 6 seconds with the other capacitor. These measured time delays satisfy the contract requirement of being adjustable from 2 milliseconds to 2 seconds.

This time delay was measured on the Breadboard Model by observing the time required for the bridge inverter to phase shift from the point of zero output to the point of maximum output. The actual rate of rise of the output voltage will also be a function of the input voltage and the load since these variables determine the amount of phase shift required to maintain the rated output voltage.

3. Overcurrent Time Delay

When an overcurrent occurs on the output terminals, the overcurrent time delay is initiated. After the overcurrent time delay has elapsed, the unit is automatically turned off and the blink-off time delay is initiated. The overcurrent circuit time delay was adjustable from 1.6

to 45 milliseconds. The blink-off circuit is synchronized with the pulse turn-off circuit that controls two transistors in one side of the inverter bridge, such that the start bus is turned off after these two transistors have been pulsed off. This synchronizing circuit prevents the possibility of saturating the power transformer during blink-off. This synchronizing circuit can also vary the effective overcurrent time delay by one-half cycle of the inverter frequency which represents a maximum added time delay of 0.625 milliseconds.

4. Blink-Off Time Delay

The blink-off time delay determines the off time of the power supply after an overcurrent fault has occurred (i. e. , the time between blink-off and the start of soft-on). A train of pulses was applied to the overcurrent sensing circuit to simulate a repetitive overcurrent condition. The operation of the start-bus (Q19) was then observed on an oscilloscope. The blink-off time delay (the off time of the start-bus) was found to be adjustable from 1 to 50 milliseconds. These measured time delays satisfy the contract requirement of being adjustable from 2 to 50 milliseconds.

5. On-Off Switch

Turning the on-off switch from the "on" position to the "off" position energizes the overcurrent trip circuit. Under this condition, the unit blinks-off after the overcurrent time delay elapsed and remained off as long as the switch was in this position.

The off switch is connected to the overcurrent trip circuit so that blink-off is synchronized with the pulse turn-off circuit as previously described.

B. STATIC LOAD TESTS

1. Output Voltage Regulation

The unit was operated into a variable resistive load. The output voltage was recorded while varying the output load from no-load to full-load and while varying the input voltage from 90 volts to 110 volts. Figure 3 shows the results of these measurements.

The measured voltage regulation satisfies the requirements of 2500 VDC $\pm 5\%$ from 30% - 100% load and 2500 VDC $\pm 10\%$ at no-load.

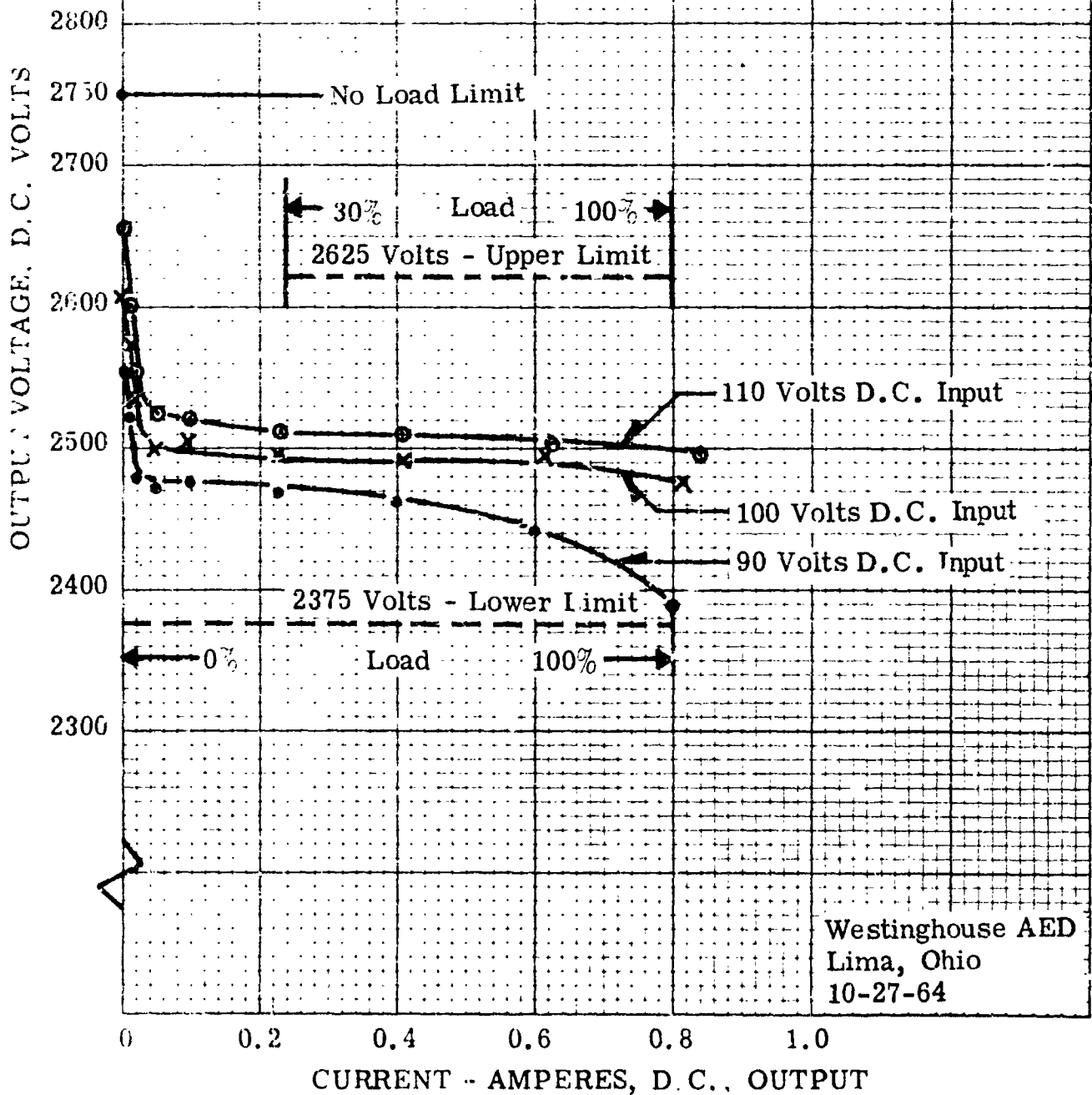
2. Efficiency

The full load efficiency exceeds the proposed minimum requirement of 85% by several percent as seen in Figure 4.

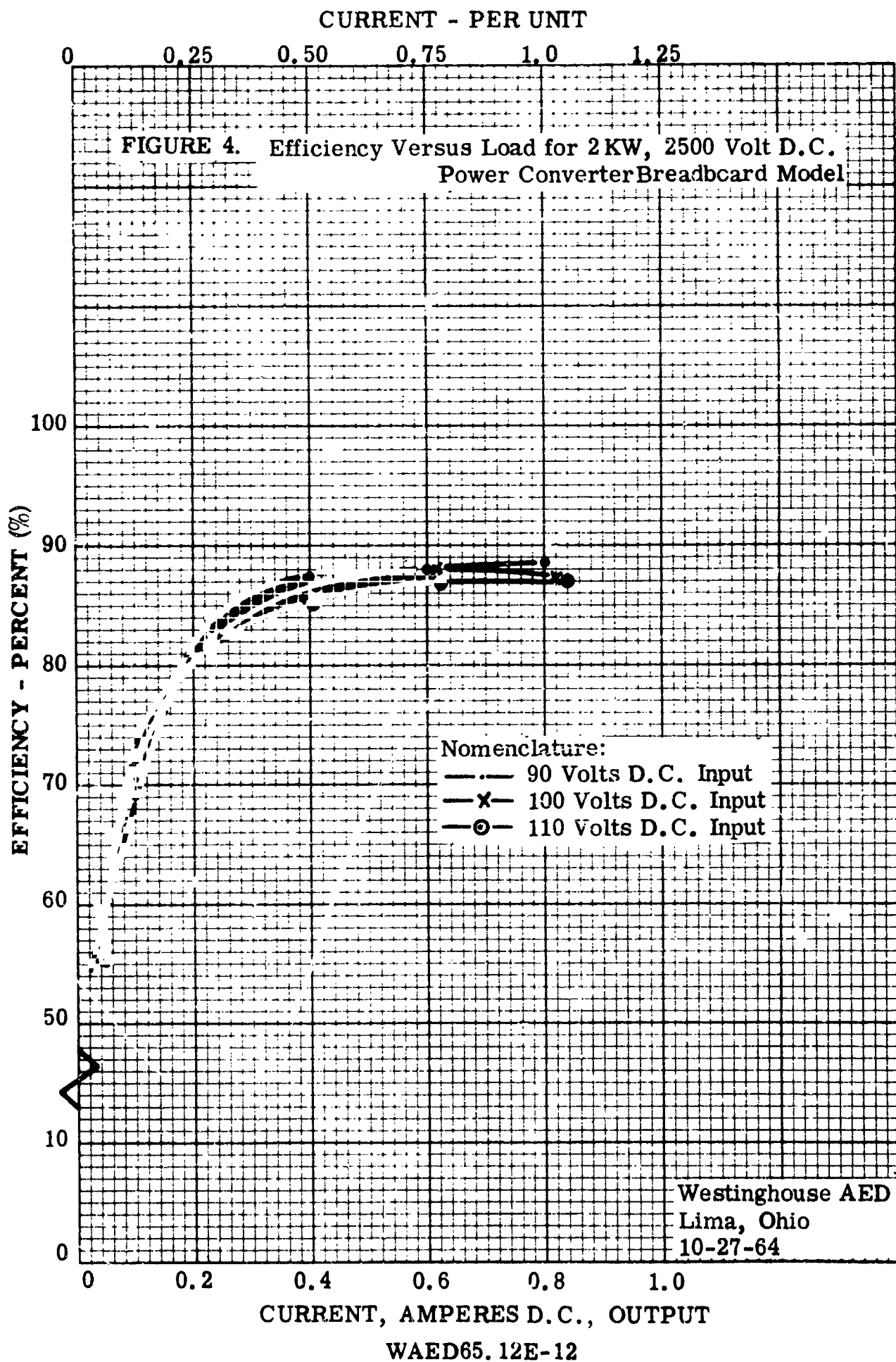
CURRENT - PER UNIT

0 0.25 0.5 0.75 1.0 1.25

FIGURE 3. Voltage Regulation Curves for 2 kW, 2500 Volt D.C.
Power Converter Breadboard Model



WAED65.12E-11



3. Output Voltage Ripple

The output voltage ripple with an input voltage of 100 VDC is as shown in Figure 5. Using a high voltage capacitor for d-c isolation and an RMS a-c voltmeter, the voltage ripple shown in Figure 5a is 18 volts RMS.

$$\text{Percent Ripple} = \frac{\text{RMS Ripple} \times 100}{\text{Nominal D-C Voltage}} = \frac{18 \times 100}{2476} = 0.73\%$$

This satisfies the contract requirements of 5% maximum ripple.

4. Input Current Ripple

The maximum limits for input current ripple are 2% RMS and 5% peak. It appeared from preliminary measurements that the input current ripple did not quite meet these requirements. The results of the Experimental Model evaluation verified these preliminary measurements.

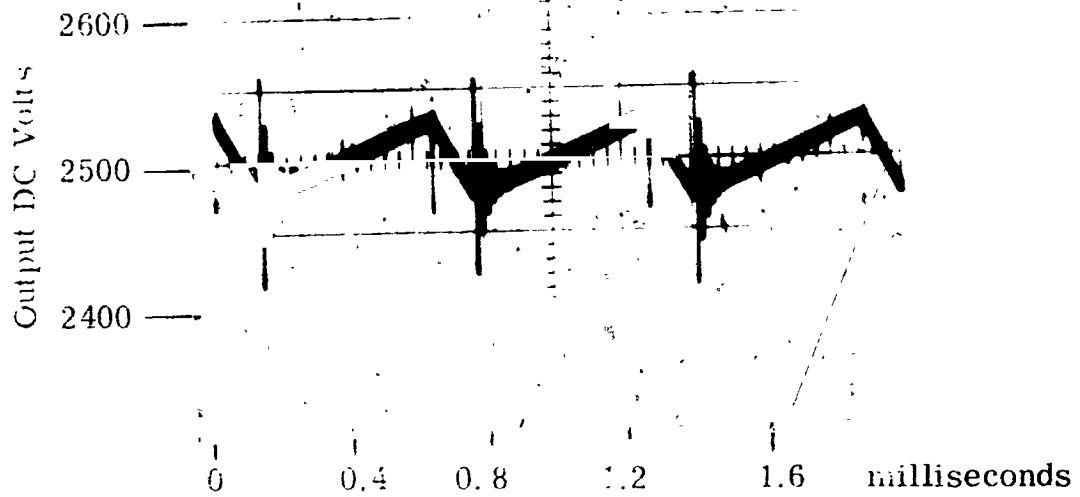
C. COMPONENT ELECTRICAL STRESS TESTS

The Breadboard Model was subjected to the application and removal of short circuits using a knife switch as the shorting device. When a short circuit was applied, the current limiting circuit limited the output current until the overcurrent time delay circuit performed its function of turning-off the start-bus. After the blink-off time delay had elapsed, the start-bus turned on and the soft-on time delay controlled the rate of rise of the output current. These successful results were not obtained until after several components failed and design improvements had been made as described below.

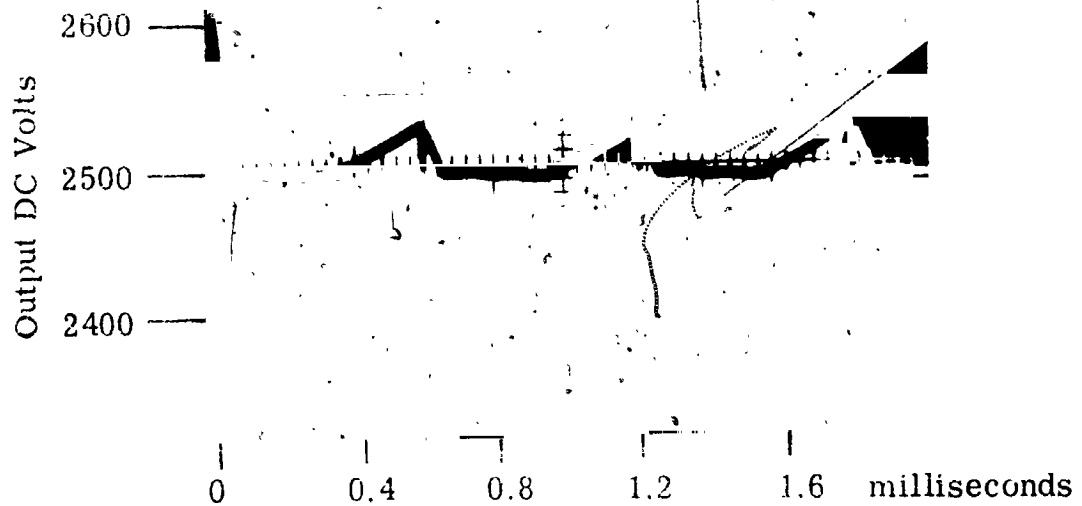
The unit then cycled off and soft-on, performing the various time delay functions as described above, until either the short circuit or the input power was removed, or until the on-off switch was turned to the "off" position.

The Breadboard Model was successfully controlled by means of the on-off switch while working into a short circuit and while working into a normal load.

To obtain oscilloscope pictures of the power transistor and output voltage transients during application and removal of short circuits, the overcurrent trip circuit was made inoperative. With this condition existing, the picture of Figure 6 was obtained. The bottom trace represents the voltage on the power supply output terminals and the top trace represents



5a. (full load)



5b. (no load)

FIGURE 5. Output Voltage Ripple

WAED65. 12E-14

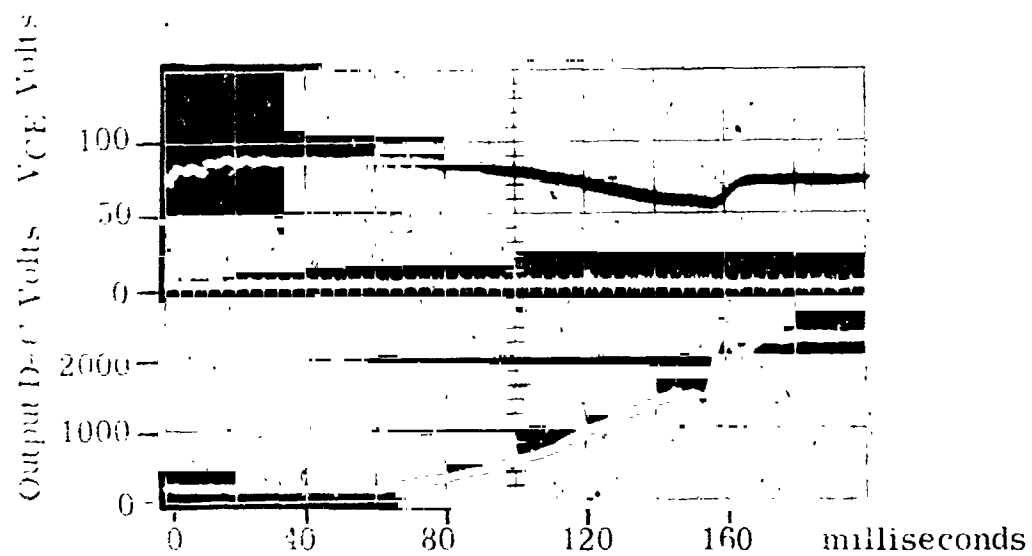


FIGURE 6 Application and Removal of a Short Circuit
(60 MS duration) with the Overcurrent Trip
Circuit Disconnected

the voltage across one of the power transistors in the bridge inverter. The picture represents a single sweep with the sweep initiated with the application of the short circuit. The short circuit condition remained on for 60 milliseconds. Upon removal of the short, the output voltage recovered within approximately 100 milliseconds. This recovery time was determined primarily by the arcing of the knife switch and the output filter rather than the soft-on circuit since the blink-off circuit was purposely made inoperative.

Using the shorting method described, it appears that the voltage stresses applied to the power semiconductor devices do not exceed the desired two-to-one safety factor. Many semiconductor voltage and current stresses were later determined, during the Experimental Model evaluation, using both a hydrogen thyatron and a vacuum relay as shorting devices. These results are described in Section V.

D. COMPONENT FAILURES AND CORRECTIVE ACTION

During the development and preliminary evaluation of the Breadboard Model, six 65-ampere silicon power transistors failed. Each failure has been attributed to a malfunction or design deficiency in the control and drive circuits. These failures are listed below along with the design improvements which corrected the causes of failure.

Failure of one power transistor was attributed to a malfunction of a gate controlled switch-type d-c chopper circuit which was originally used to provide control power to the unit. Due to the unreliability of the gate controlled switch in this particular circuit, a new chopper circuit was designed using a transistor as the switching device. The new chopper circuit operates successfully and is shown in the schematic diagram, Figure 2. It consists of a non-symmetrical Royer oscillator driving chopper transistor, Q37.

Failure of one power transistor was attributed to frequency modulation of the reference oscillator in conjunction with an erroneous signal from the current transducer in the overcurrent sensing circuit. This was corrected by placing a resistive load (R81) on the output winding of the oscillator transformer (T9) and by changing the location of the filter capacitor in the overcurrent sensing circuit so that the transducer operates into a resistive load.

Failure of two power transistors was attributed to the simultaneous failure of transistors Q12 and Q13 in the Jensen oscillator when a short circuit was applied to the output terminals. The application of the short circuit caused the rapid discharging of the output filter capacitors through the current sensing transducer (AR1). This in turn overloaded

the transducer driving source which is the Jensen oscillator. This problem was corrected by placing a redundant connected resistor (R90-R97) in series with the output filter capacitor to limit the surge current to 3 PU, and by placing commutating diodes (CR60 and CR61) around the transistors in the Jensen oscillator to commute the lagging current caused by the transducer.

The last failure of two power transistors was not associated with the failure of a particular control or drive circuit function. However, improvements were made in three circuit areas that were considered possible causes of the last failure which occurred in the Breadboard Model.

1. The commutating diodes (CR45-CR48) in the bridge inverter were changed from Zener diodes to 35 ampere high speed rectifiers. This reduces the crowbar effect when a power transistor turns on into a diode that has not recovered its reverse blocking capability after carrying commutating current.

2. The second design improvement consisted of placing clamping diodes (CR43, CR44, CR57 and CR58) around the controlled current feedback transformer (CCFT) turn-off winding. This provides a low impedance path for any pick-up in the CCFT that may tend to turn on a transistor that is normally off.

3. The third design improvement was the addition of the circuit (Q35) that synchronizes the blink-off of the start bus so that it is accomplished after the two power transistors in one side of the bridge inverter have been pulsed off by the pulse turn-off circuit. Operation of the off switch is also synchronized with the pulse turn-off circuit by applying a false signal to the overcurrent time delay circuit.

All test results recorded in this section were obtained after these changes were incorporated in the unit. For example, the output voltage ripple was recorded after placing the 1000-ohm resistor in series with output filter capacitors. The Breadboard Model operated more than the minimum requirement of 10 hours without failure after these changes were incorporated.

IV. POWER TRANSISTOR EVALUATION

The 65-ampere silicon power transistors (STC Type 2118) were investigated to evaluate their performance when operating in a test circuit and to compare this with data obtained while operating in the inverter circuit. The following parameters were investigated:

1. Gain - h_{FE}
2. Base-to-Emitter Characteristics
3. Saturation Resistance
4. Switching Speed
 - a. Operating into a resistive load with fixed base drive.
 - b. Operating in the power supply with current feedback base drive.
5. Losses when operating in the power supply.

These test results are presented in this report because of the recent introduction of the transistor to the power semiconductor market and because of its effect on the design and operation of the power converter.

A. CURRENT GAIN

The d-c current gain (h_{FE}) of the 65-ampere silicon power transistors was measured using a Tektronix, Type 575, transistor-curve tracer and a Tektronix, Type 175, transistor-curve tracer, high current adapter. The current gain was measured with up to 50 amperes collector current. For the four transistors that were tested, the current gains were 8.1, 9.0, 7.8 and 7.6 at 50 amperes collector current. This is less than the manufacturer's published minimum limit of 10. Figure 7 shows the family of curves obtained on the transistor-curve tracer for one particular transistor. All figures included are for this particular transistor.

The base drive current transformers in the power converter have a turns ratio of seven. Therefore, adequate base current is provided to keep the transistors saturated with collector currents up to 50 amperes since all transistor current gains exceeded seven.

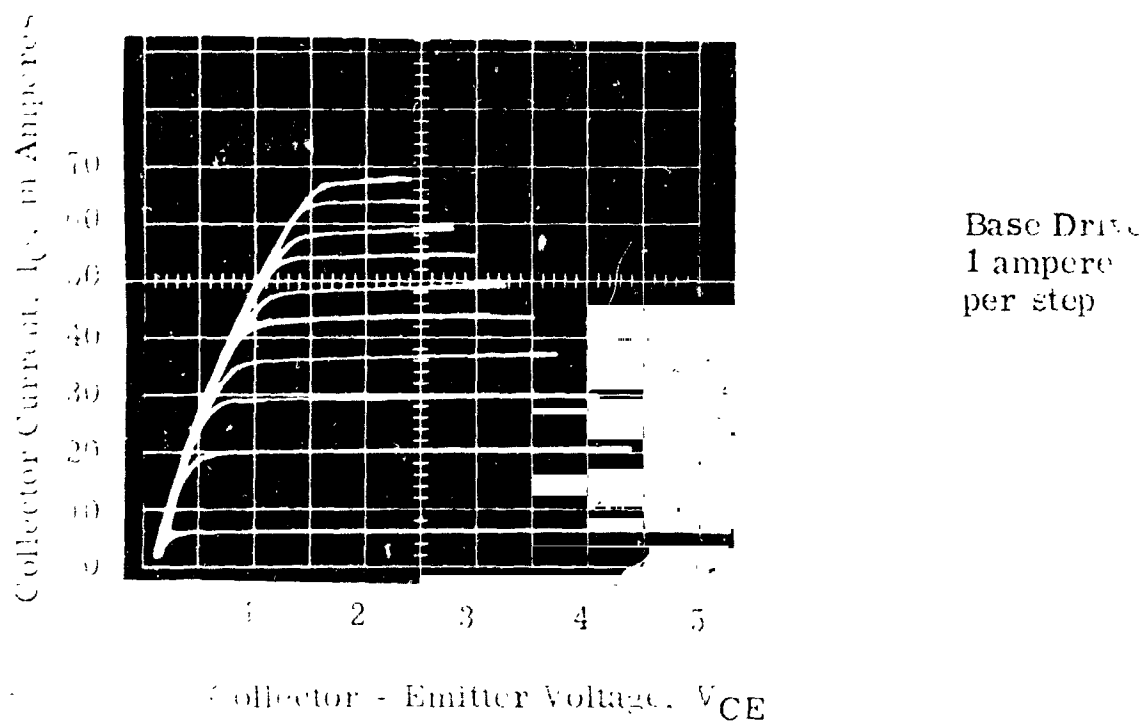


FIGURE 7 Common-Emitter Collector Characteristics of STC 2118

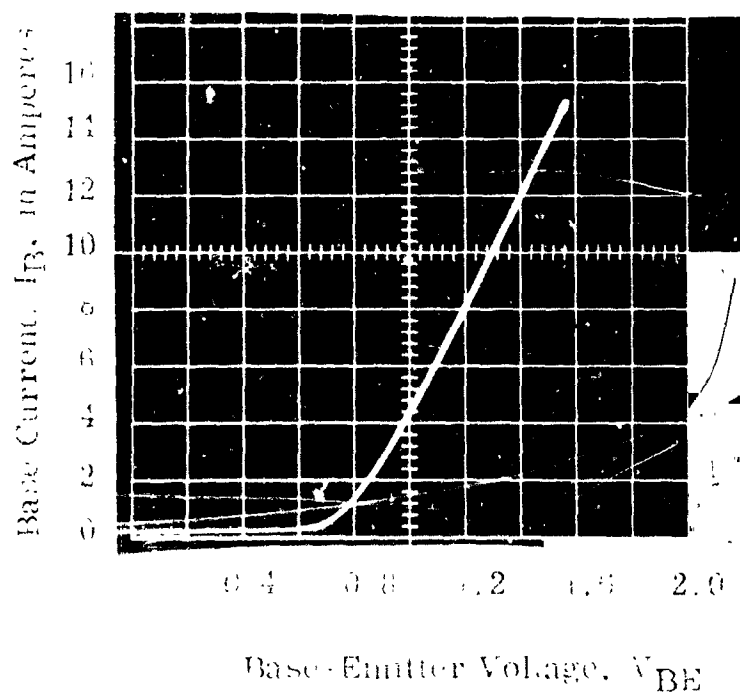


FIGURE 8 Base-Emitter Characteristics of STC 2118

B. BASE-TO-EMITTER FORWARD DROP

The base-to-emitter forward drop is an important parameter when using the controlled-current, feedback transformers. This base-to-emitter forward drop contributes to the losses in the power transistor (base voltage x base current). This forward voltage drop, in conjunction with the transistor current gain (h_{FE}), also indicates the size of the controlled current feedback transformer. The base-to-emitter forward drop ranged from 0.96 to 1.07 volts at the condition of full load on the power supply for the four transistors. Figure 8 shows the forward base emitter characteristics of the transistor as obtained from the Tektronix transistor-curve tracer.

C. SATURATION RESISTANCE

The saturation resistance at 50 amperes collector current was obtained from the family of curves that were used to measure the gain. The saturation resistance for the four units was 0.021, 0.010, 0.017 and 0.033 ohms. The saturation resistance is an important parameter affecting the transistor losses and the power supply efficiency. One of the four transistors exceeded the published maximum limit of 0.03 ohms.

D. SWITCHING SPEED

The switching speed of the transistor is another important parameter affecting the transistor losses. The switching times of the transistors were measured with the transistors operating into a resistance load in a test circuit. The switching times were also measured with the transistor operating in the power supply under the condition of 1 PU load. The switching times of the four transistors, in the test circuit were as follows:

	#1	#2	#3	#4
Turn-on Time (t_r)	8 usec	6 usec	9 usec	12 usec
Turn-off Time (t_f)	6 usec	6 usec	3 usec	7 usec

The current at the condition of turn-on was approximately 36 amperes for all units and the current at the condition of turn-off was approximately 26 amperes for all units. Figure 9 shows the turn-on time of a transistor in the test circuit and Figure 10 shows the turn-off time. Figure 11 is a schematic diagram of the test circuit. Transistor Q2 is the one under test, transistor Q1 is a high speed transistor with switching time of 1 usec or less and relay contact K is a mercury wetted, relay contact operating at 60 cps. All resistors are non-inductive, carbon composition, resistors. A brine solution was used for the power transistor load resistor.

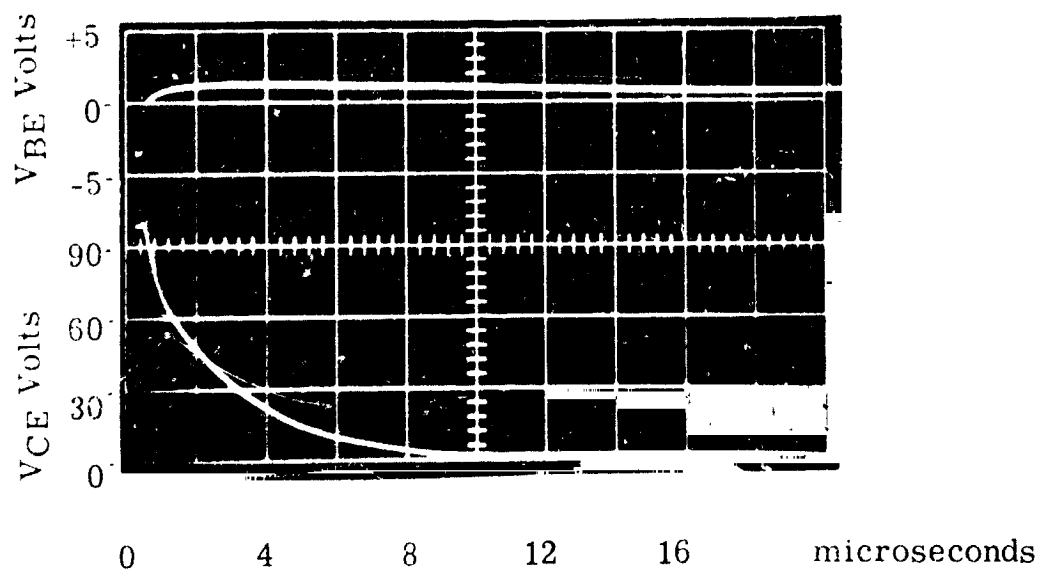


FIGURE 9. Transistor Turn-On Transient with 36 Ampere Load in Figure 11 Test Circuit

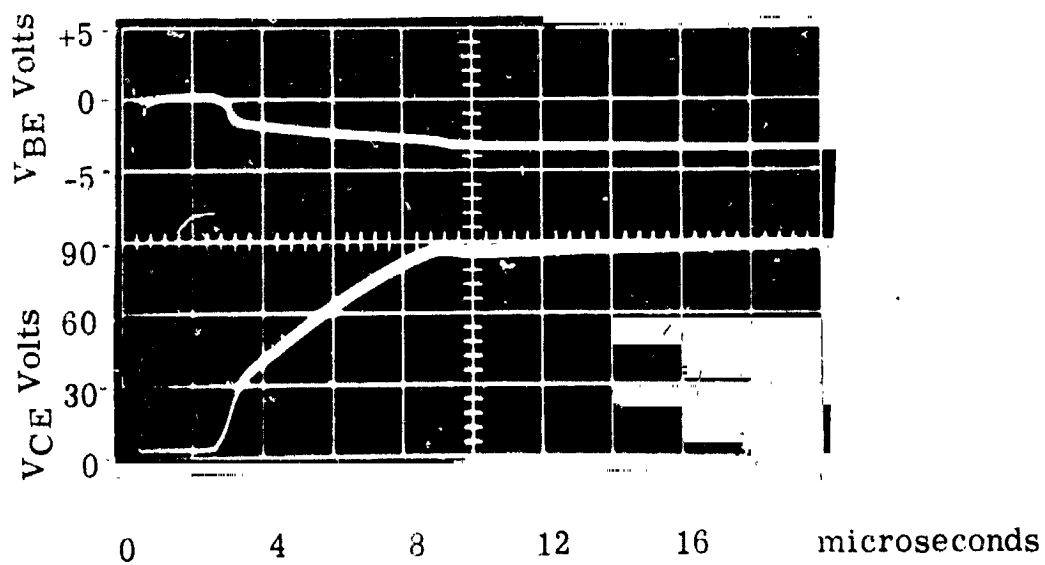


FIGURE 10. Transistor Turn-Off Transient with 26 Ampere Load in Figure 11 Test Circuit

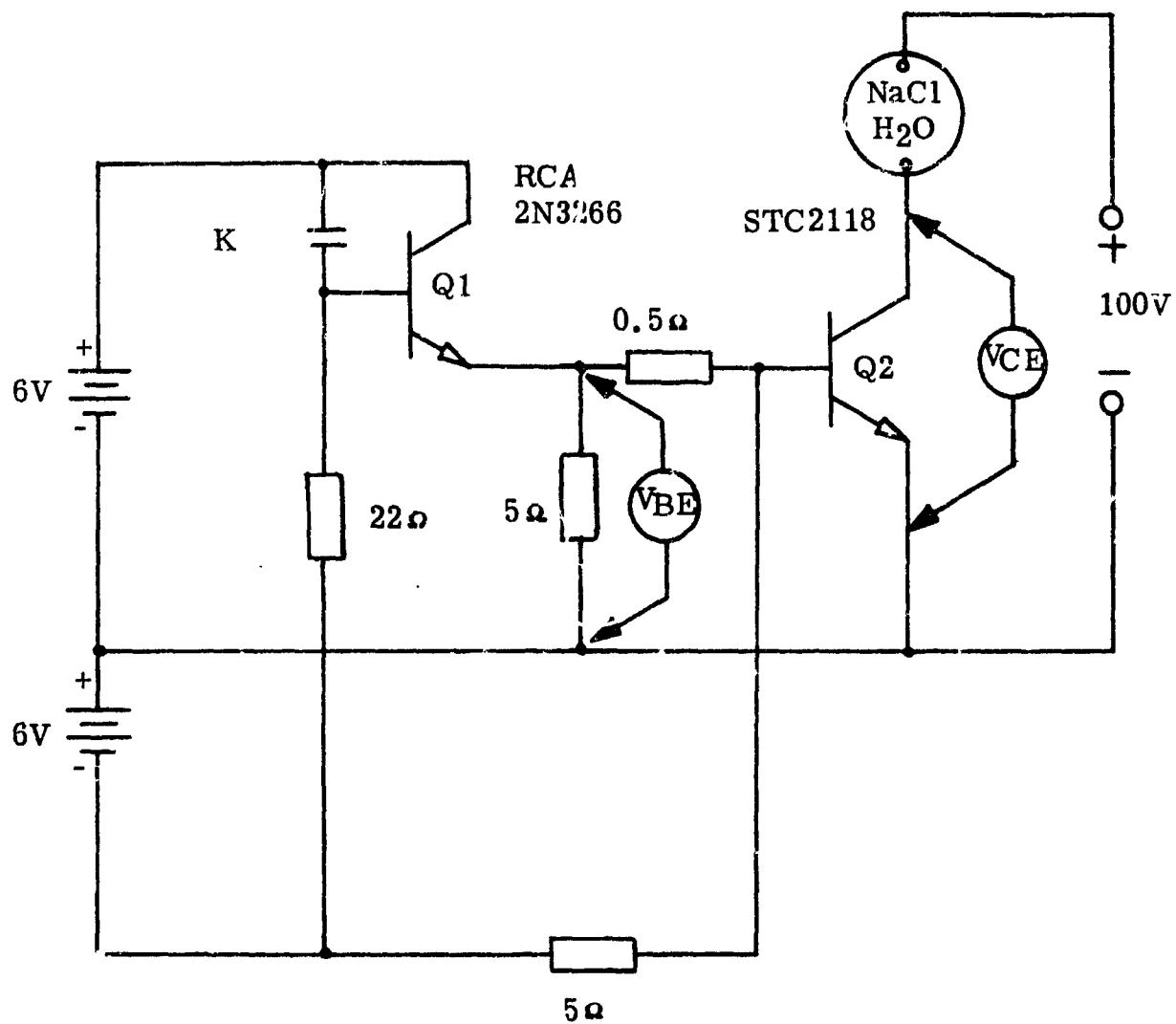


FIGURE 11. Test Circuit for Measuring Transistor STC 2118
Switching Speed

Figure 12 shows the turn-on time of the same transistor when operating in the power supply and Figure 13 shows the turn-off time. Figure 13 shows the current waveform through this same transistor with 1 PU load on the power supply.

Figure 9 and Figure 12 cannot be compared directly in an attempt to determine the effect that the controlled current feedback transformer (CCFT) base drive circuit has upon transistor switching speeds because of load differences. With circuit inductance of the power converter, the current through the transistor requires about 18 usec to reach its maximum value (see Figure 14). This is a much less severe loading than in the test circuit. Figures 12 and 13 do indicate that the transistor switching speed is much faster while operating in the power supply than while operating in the test circuit. In the converter, turn on time (t_r) is approximately 2.8 microseconds and turn off time (t_f) is approximately 1.6 microseconds. These results indicate that actual switching losses are at least 50% less than the switching losses that were initially calculated for the purpose of selecting the optimum inverter operating frequency. These results will raise the optimum inverter frequency and lower the total system weight.

The power transistors turn on faster in the converter than in the test circuit because circuit inductance decreases the collector current rate-of-rise. The most probable reason the power transistors turn off faster in the converter than in the test circuit is because the transistor base-to-emitter junction is strongly reverse biased during the turn-off period by the CCFT base drive circuit.

E. LOSSES

Figure 15 was obtained by causing a power transistor to dissipate known amounts of power on a given heat sink in still air. The power supply was then operated at full load until the temperatures of the power transistors stabilized. From the measured temperature rise of 34°C, it was determined by using Figure 15 that the full load losses of transistor Q1, R1, CR45, CR49, CR50 and T2 are 28 watts. All of these items are mounted on the same heat sink. With a few calculations, this loss is divided as follows:

Transistor Q1	20.0 Watts
R1, CR49, CR50	2.8 Watts
CR45	0.2 Watts
T2	3.0 Watts
Total	28.0 Watts

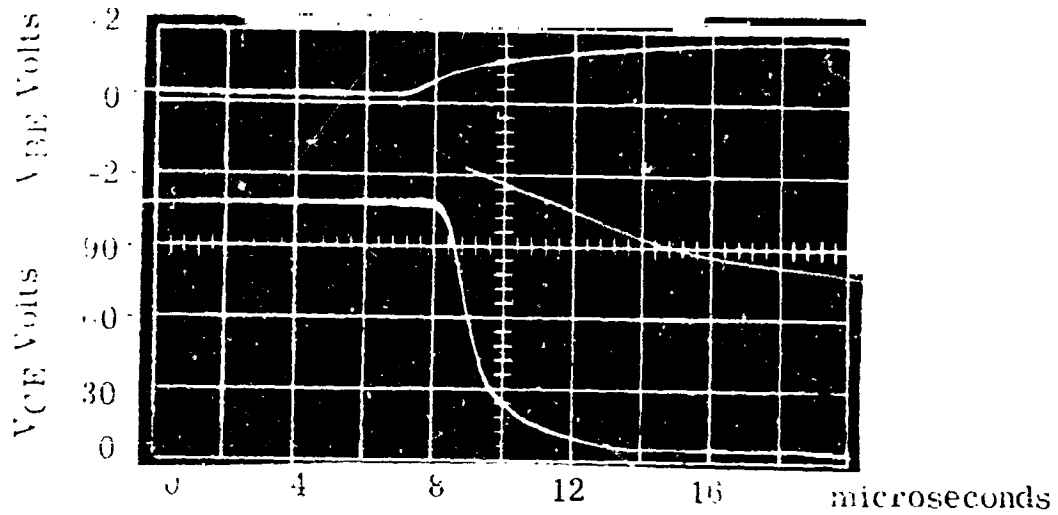


FIGURE 12 Transistor Turn-On Transient in Power Supply
with 30 Ampere Collector Current
Shown in Figure 14

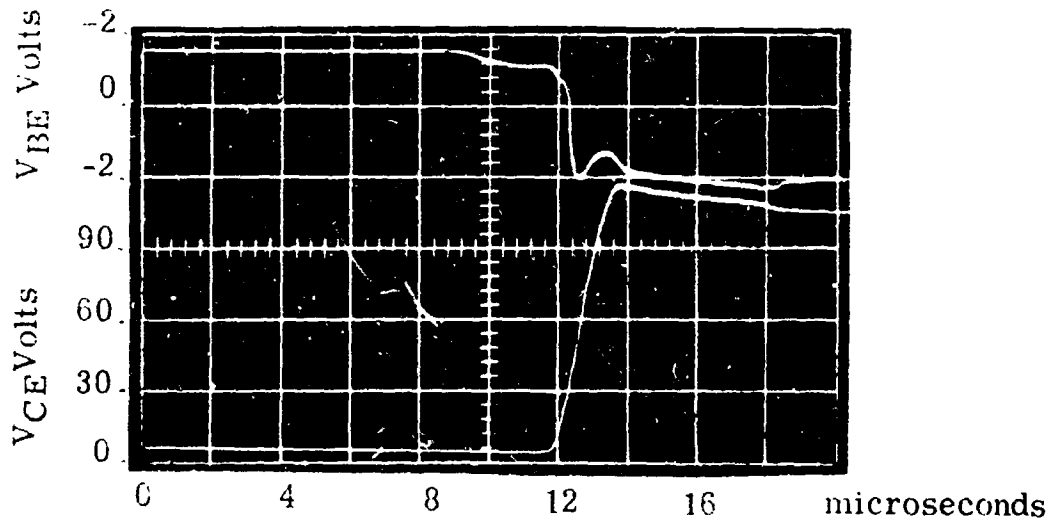


FIGURE 13. Transistor Turn-Off Transient in Power Supply
with 22 Ampere Collector Current Shown
in Figure 14

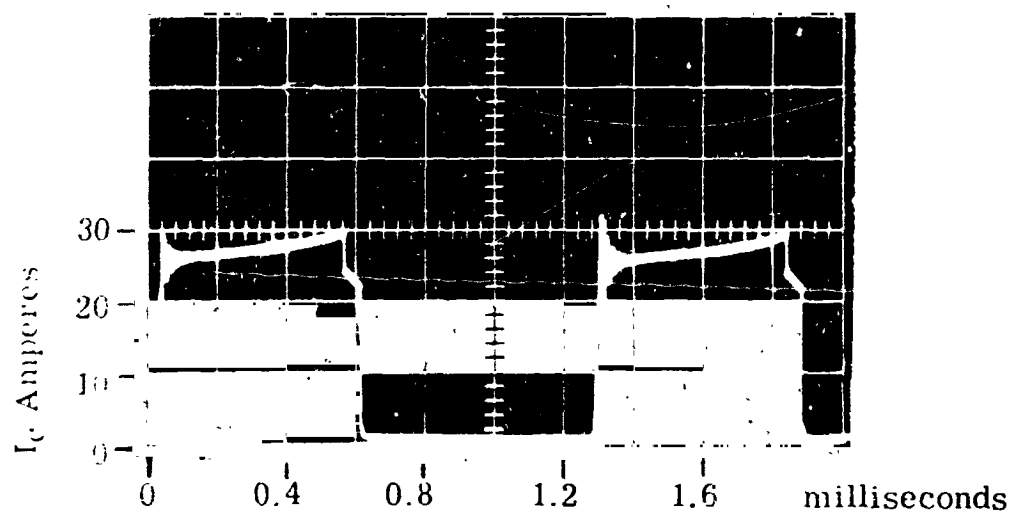


FIGURE 14. Transistor Collector Current with 1 PU
Load on the Power Supply
(T & M Research Products Shunt Type F-500-2)

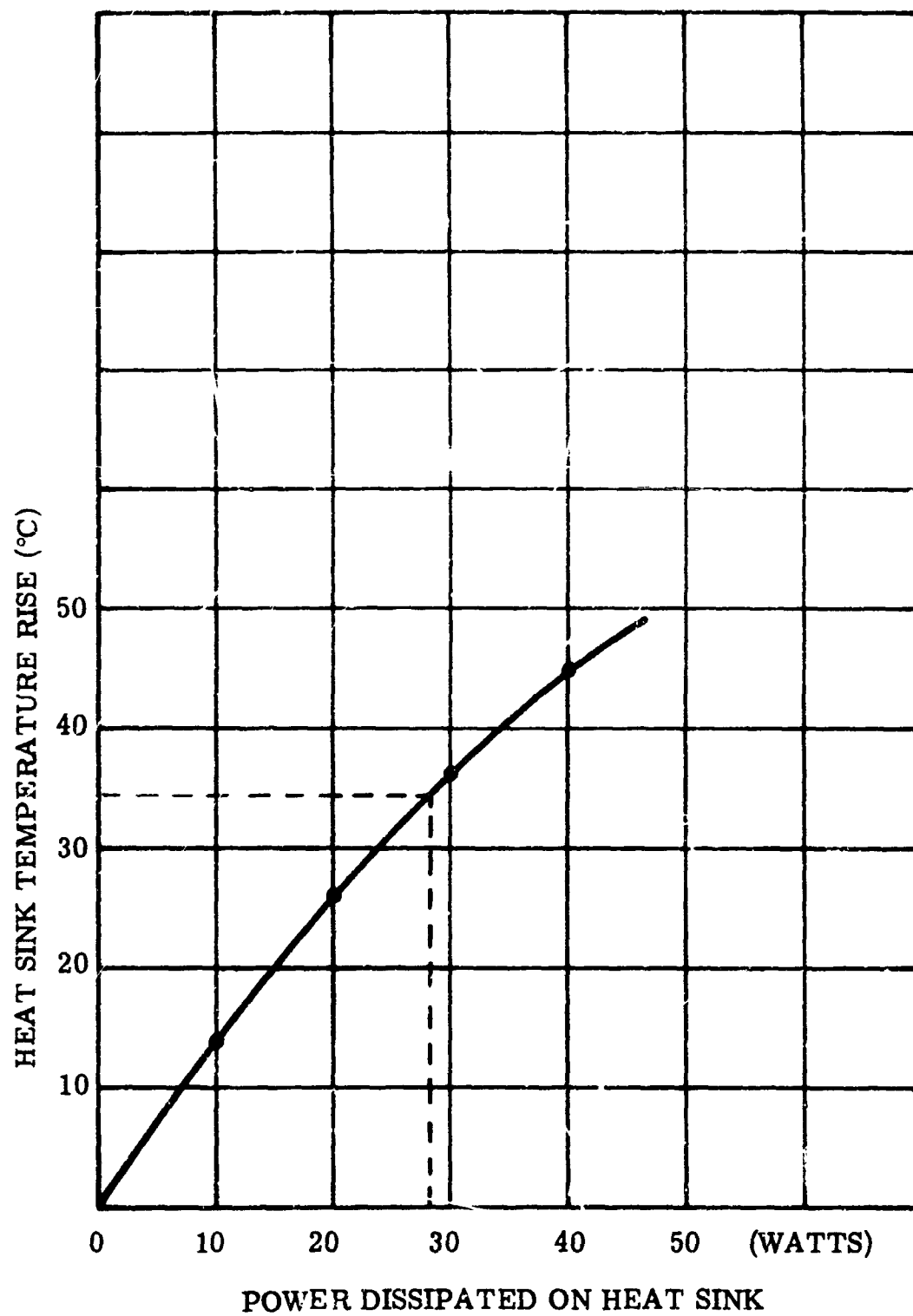


FIGURE 15. Calibration of Transistor Heat Sink

WAED65.12E-26

The losses of power transistor Q1 are much lower than originally calculated. The original calculations were based on the best data available at the time and indicated the maximum turn-on time (t_r) would be 15 microseconds, maximum turn-off time (t_f) would be 9 microseconds, and the maximum saturation resistance would be 0.03 ohms. Using these maximum values, the calculated full load switching loss at 800 cps was 22 watts per transistor. The remaining transistor losses (leakage, base, and conductor) are essentially unchanged and amount to an additional 11.8 watts per transistor. The switching losses for an actual transistor operating in the inverter are therefore only $22.0 - 11.8 = 10.2$ watts. The fact that these power transistors appear to have approximately 50% lower switching losses than anticipated will allow the inverter operating frequency to be increased and the overall system weight to be decreased.

By using this information on transistor switching losses to revise Figure 1, it appears that an inverter frequency of 1200 cps would result in minimum system weight. This change in frequency would reduce the inverter component weight approximately 5 pounds and reduce the system weight (including inverter, solar cell array, and waste heat radiator) approximately 19 pounds. Additional weight reduction is possible by changing the performance requirements as discussed in Section VI.

V. EXPERIMENTAL MODEL EVALUATION

The mechanical design of the Experimental Model was determined by consideration of safety and ease of evaluation. The rear view of the model, given in Figure 16, shows that all control circuit components are easily accessible and are identified on externally mounted terminal strips. The power transistors and commutating diodes are mounted on four vertical heat sinks seen in the foreground. All high voltage components, including the output transformer, rectifier and filter, are mounted between the two side chassis and protected by a perforated aluminum cover. Input and output connectors, input and output voltmeters, output voltage adjustment potentiometer, the soft-on, blink-off and overcurrent time delay adjustment potentiometers, and the low-level on-off switch are all mounted and accessible on the standard 14 inch x 19 inch x 1/8 inch front panel.

The basic electrical design of the Experimental Model is the same as the Breadboard Model which has been described. During the preliminary testing of the Experimental Model, however, several design improvements were made. The design improvements and test results will be presented in this section of the report.

A. PRELIMINARY CHECKOUT OF EXPERIMENTAL MODEL AND DESIGN IMPROVEMENTS

1. Soft-On Circuit Design Improvement

The soft-on circuit operated properly and caused the output voltage to rise exponentially at rates which could be adjusted from about 2 to 5000 milliseconds. It was noted, however, that the time delay capacitor C12 required approximately 20 ms to be recharged. This time exceeds the minimum blink-off time delay by a factor of 10. To assure that the soft-on capacitor C12 will be recharged completely during the minimum blink-off time delay, the soft-on circuit was redesigned as shown in the revised schematic diagram, Figure 2.

2. Overcurrent Time Delay Circuit Design Improvement

It was next noticed that the converter would not blink-off after the application of an overload or short circuit when potentiometer R45 was at its maximum setting. Insufficient current passed through R45, R46, Z10 and R87 into the gate of CR25 to turn it on during the short period when Q35 was not conducting. To correct this situation, R45 was decreased from 50K to 20K ohms and R85 was increased from 10K to 20K ohms. The latter change increased the reverse bias of transistor Q35 during the discharging periods of capacitor C16.

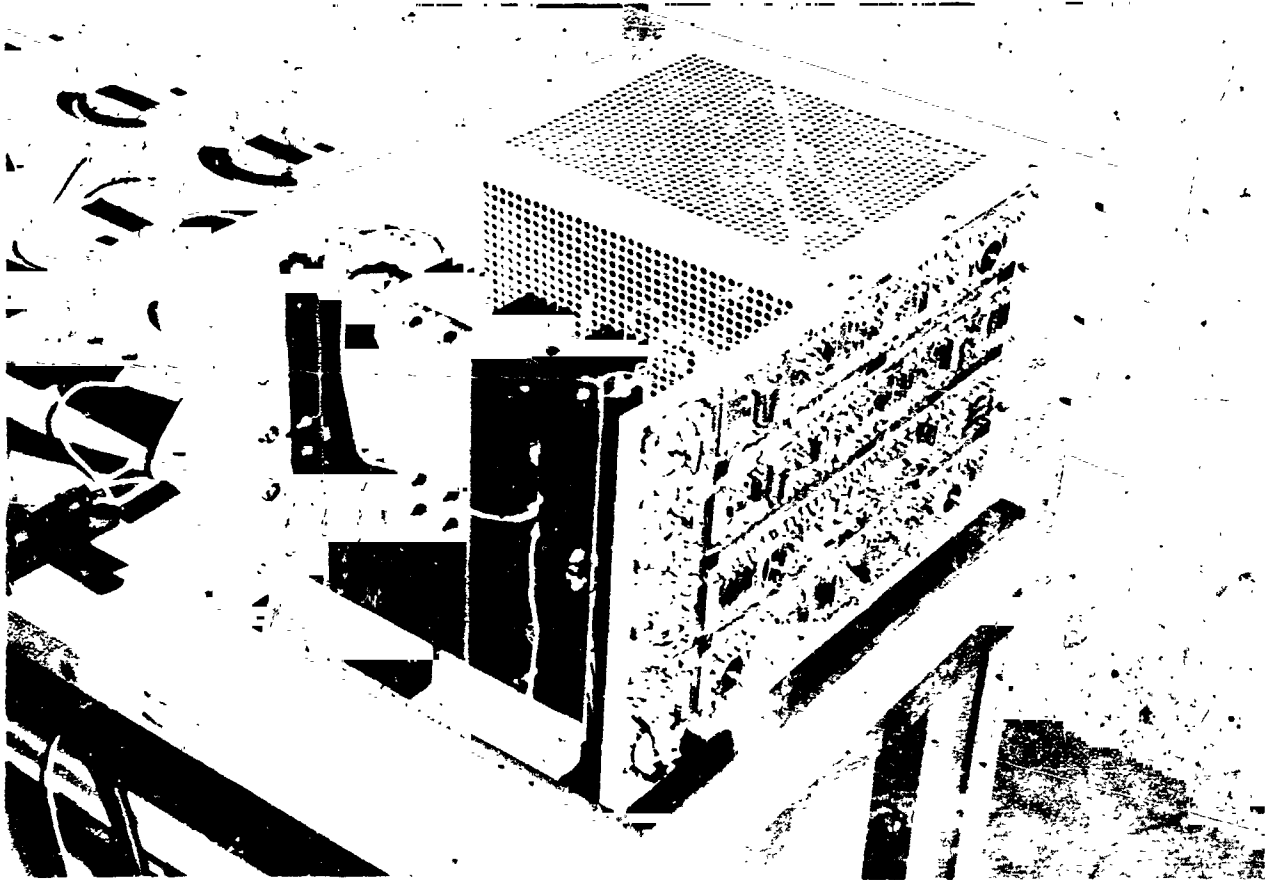


FIGURE 16. Rear View of Experimental Model

3. Blink-Off Time Delay Circuit Design Improvement

Next, it was noted that the converter would blink-off on application of short circuit but it would not automatically turn on after the blink-off time delay except for minimum settings of R39. This was caused by collector leakage current through transistor Q21 which prevented the emitter of unijunction transistor Q20 from reaching the breakdown level. This leakage current was adequately reduced by reducing the base-to-emitter resistor, R67, from 51K to 1K ohms.

4. Overcurrent Sensing Circuit Design Improvement

It was observed that the current limiting level was lower than the level of output current which would cause the converter to blink-off. Therefore, it was possible to have an overcurrent load condition which would not cause the supply to blink-off. To correct this condition, R49 was reduced from 51K to 10K ohms. This change increased the base current to transistor Q24 so that it turned on during output current-limiting conditions.

5. Power Transistor Failures

Several power transistors failed during the preliminary checkout of the Experimental Model. However, it was determined that these failures were caused by a wiring error, defective control component (Z5), and incorrect oscilloscope connections. None of the failures was caused by design deficiencies, and no design changes resulted from these failures. After the preliminary checkout, no components failed during the entire evaluation of the Experimental Model which included static load tests, component electrical stress tests, and a thirteen hour endurance test.

B. STATIC LOAD TESTS

The power converter and load simulator were connected together and to meters and lead-acid batteries. The test setup is shown in Figure 17 with the power converter on the left, the load simulator and recording oscillograph on the right, and the laboratory meters (1/2%) in the center. The load simulator was assembled in accordance with the contract requirements and consists of a vacuum triode (RCA Type 7C24/5762) for variable resistive loads and a hydrogen thyatron (Amperex Type 6268) and vacuum relay (Eimac Type VS-2) for application of short circuit transients to the power supply. A Tektronix Type 533 Oscilloscope with a Type CA Dual Preamplifier was used to obtain all oscilloscope photographs.

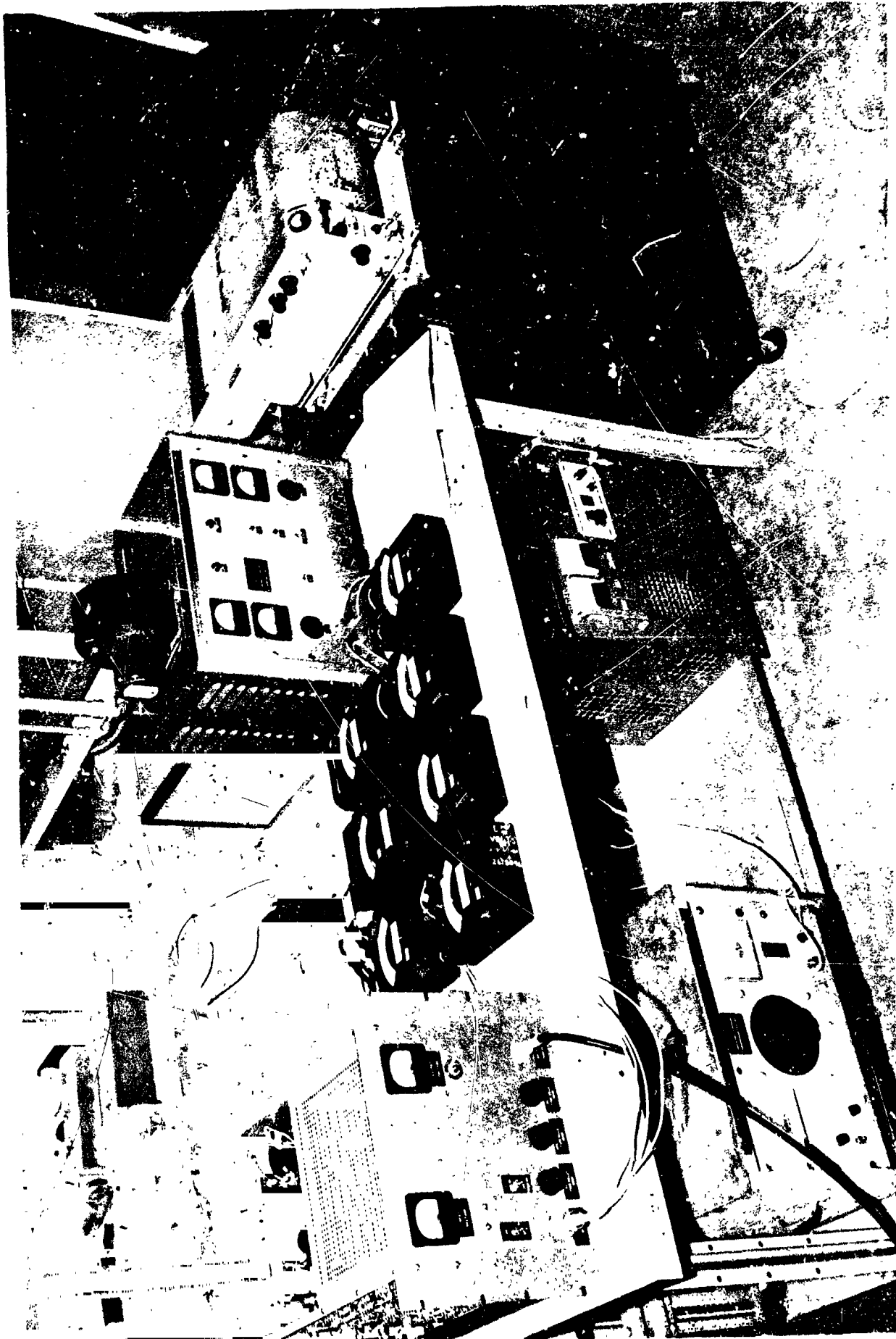


FIGURE 17. Laboratory Setup for Static Load and Electrical Stress Tests

WAED65. 12E-31

1. Soft-On Time Constant Range

The test results, given on Figures 18 and 19, indicate a maximum soft-on time constant of 3000 milliseconds and a minimum soft-on time constant of 5 milliseconds. (The significant time constant for power converters is defined as the time required for the output voltage to increase from zero to rated output voltage of 2500 volts). The contract scope of work specifies a range of 2 to 2000 milliseconds. The minimum limit of 2 milliseconds was not met because of output filter constants and not because of a control circuit deficiency. Output filter constants were determined by short circuit and current limiting requirements of the contract and could not be changed to decrease the minimum soft-on time constant from 5 to 2 milliseconds.

2. Output Voltage Regulation and Efficiency

The maximum conversion efficiency of 87.6% occurred at rated load and rated input voltage. The output voltage regulation was within the limits specified in the contract scope of work. The converter output voltage is plotted as a function of load on Figure 20. The converter efficiency is plotted as a function of load on Figure 21.

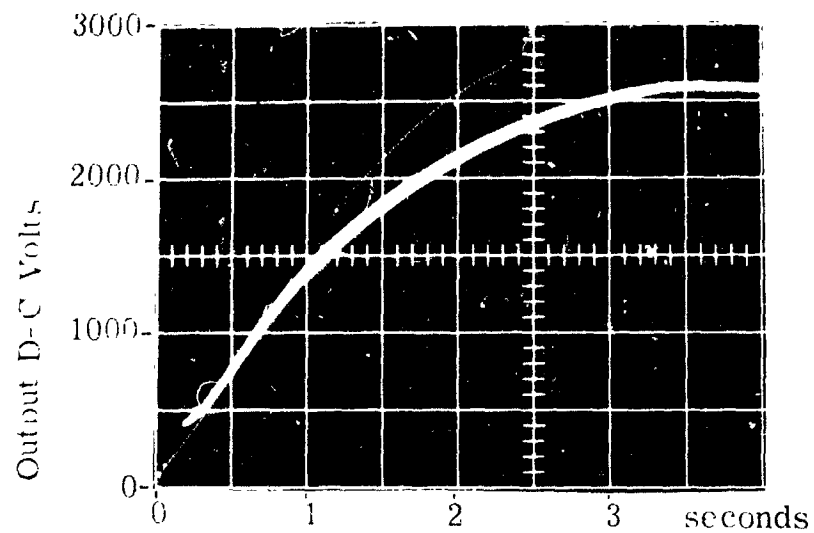
3. Input Current Ripple

The input current ripple magnitude was determined by observing the voltage across a T & M Research Products current viewing resistor. Test results are given on Figure 22 and indicate that the maximum peak-to-peak input current ripple is approximately 3 amperes. Stated another way, the peak input current exceeds the nominal input current, 22 amperes at full-load, by 1.5 amperes or 6.8%. This exceeds the 5% maximum specified in the contract scope of work but could easily be corrected by increasing the size and weight of the input filter, L1 and C1. The NASA Project Manager advised that the input filtering method had been demonstrated satisfactorily and revising the Experimental Model to meet the 5% limit would not be required.

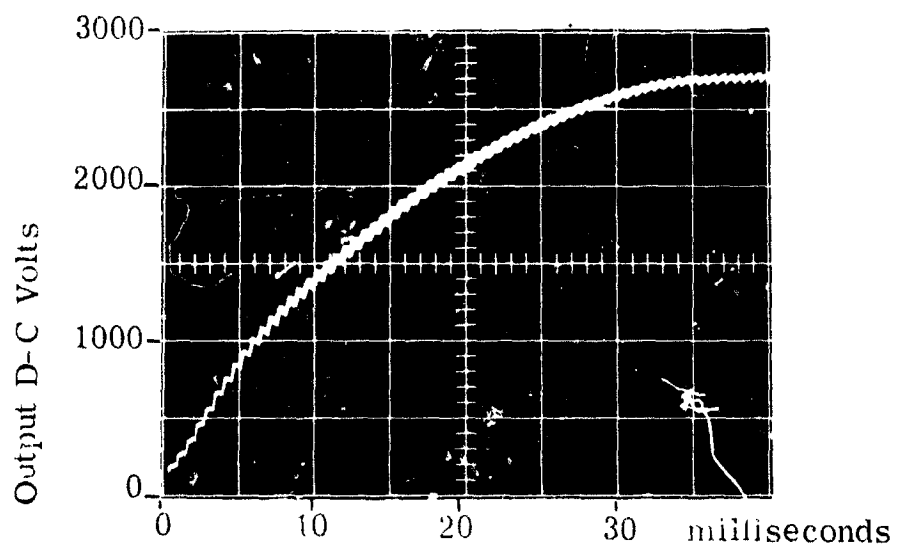
The input current ripple magnitude determined during the previous Breadboard Model evaluation was not considered sufficiently accurate because a T & M Research Products non-inductive current viewing resistor was not available at that time.

4. Output Voltage Ripple

The maximum output voltage ripple is 10 volts rms. This is 0.4% of the nominal d-c voltage and is well below the 5% allowed by the contract scope of work. Again, the output filter constants were determined by the current limiting and short circuit requirements. It is,

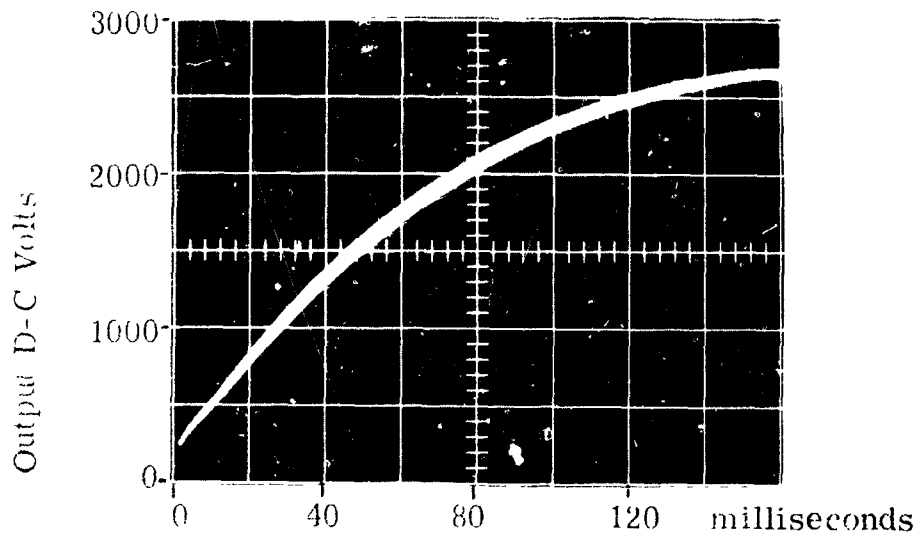


1. Output Voltage Rise with R55 = 100K Ohms

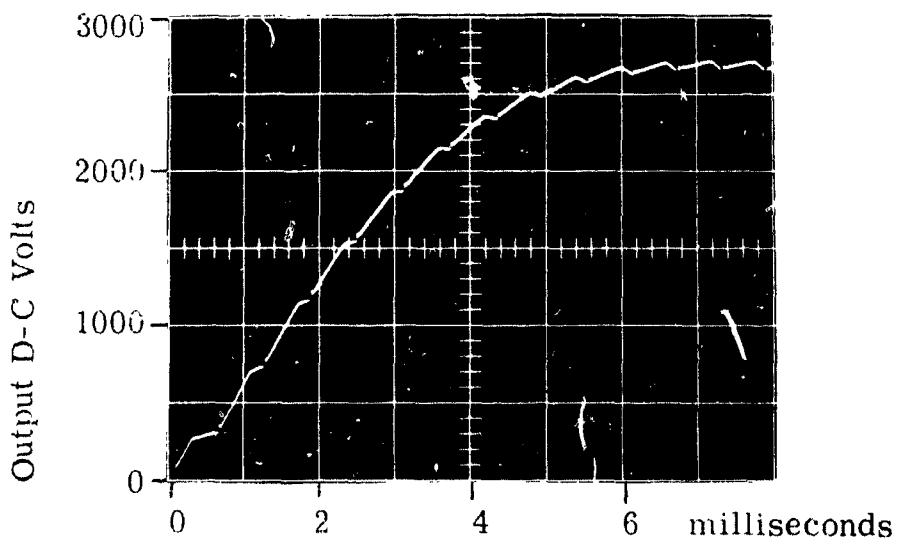


2. Output Voltage Rise with R55 = 0 Ohms

FIGURE 18. Soft-On Time Constant Range with 22 MFD Capacitor C12



3. Output Voltage Rise with $R_{55} = 100K$ Ohms



4. Output Voltage Rise with $R_{55} = 0$ Ohms

FIGURE 19. Soft-On Time Constant Range with 1 MFD Capacitor C12A

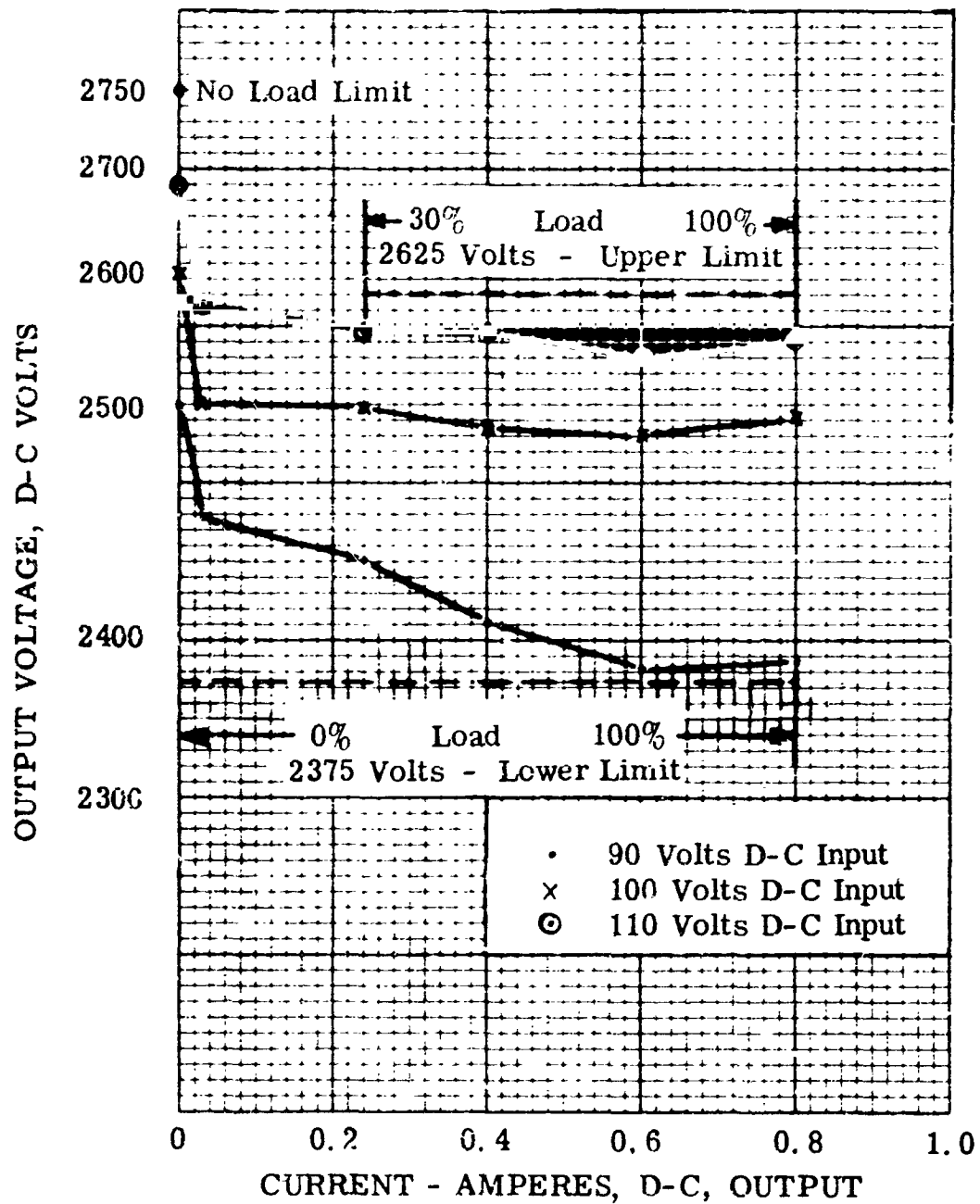


FIGURE 20. Experimental Model Output Voltage Plotted as a Function of Load

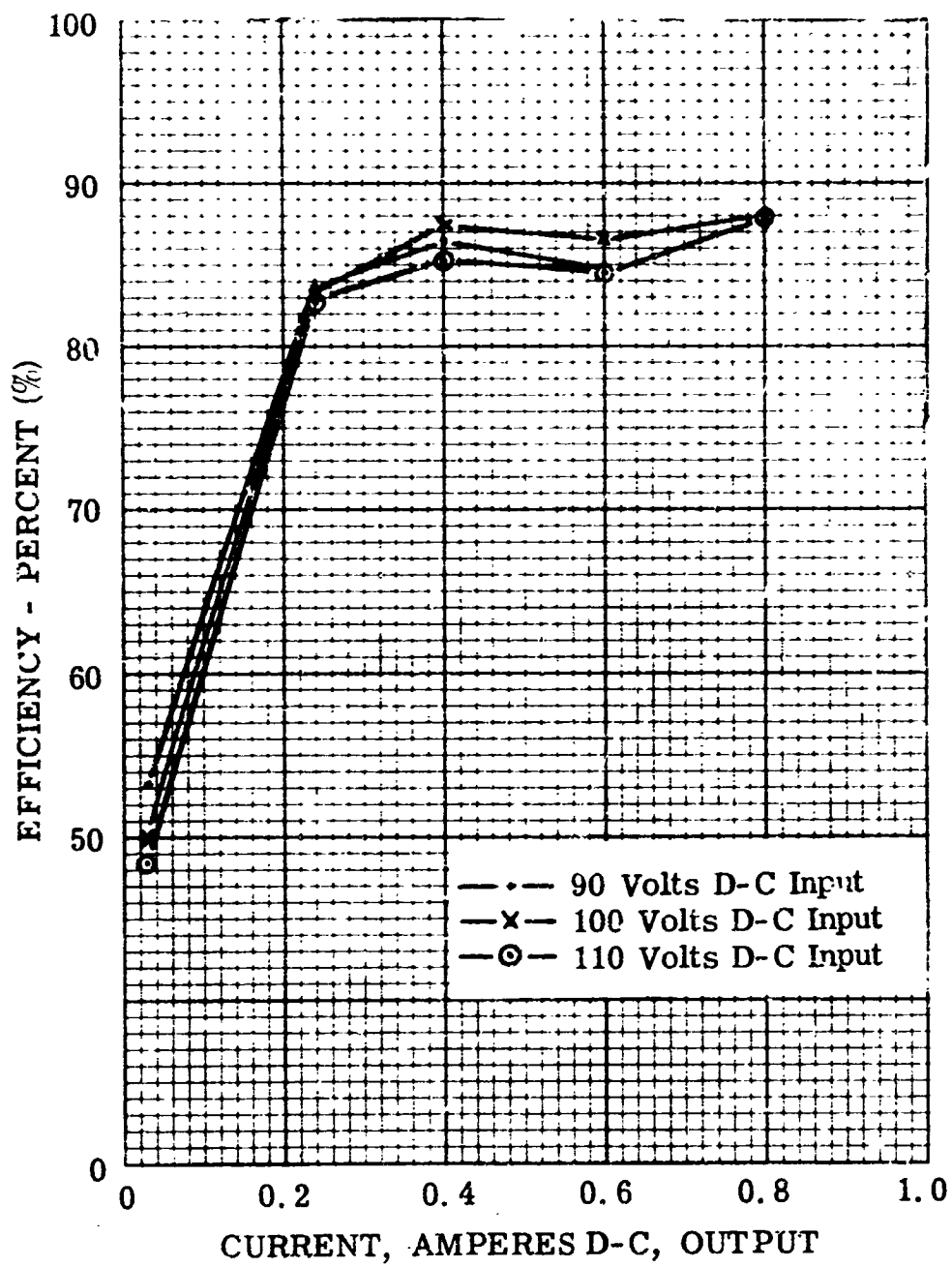
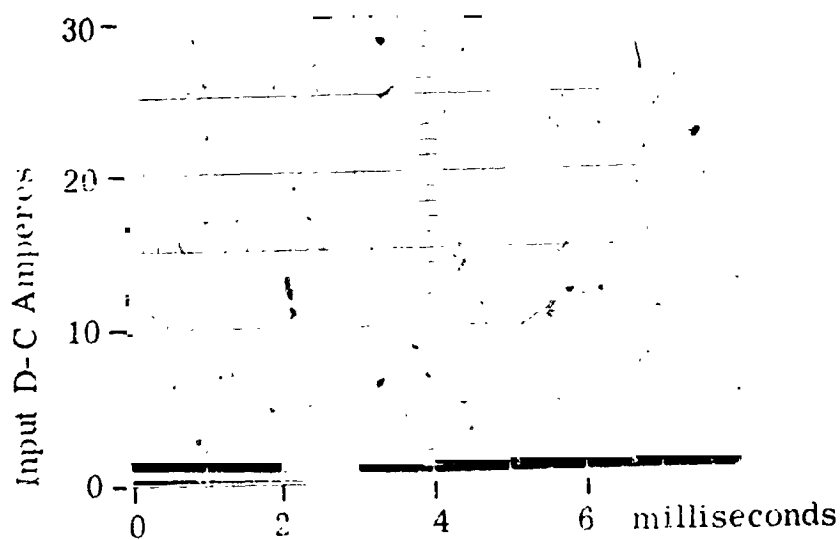


FIGURE 21. Experimental Model Efficiency Plotted as a Function of Load

WAED65.12E-36



5. Full-Load Input Current



6. No-Load Input Current

FIGURE 22. Input Current Ripple with Full-Load and No-Load on the Experimental Model

therefore, not possible to reduce them further in accordance with the allowed 5% ripple.

C. COMPONENT ELECTRICAL STRESS TESTS

As outlined in the contract scope of work, "a design objective, but not a requirement, for the Experimental Model is a minimum safety factor of two for current and voltage for semi-conductors". Electrical stress test data were obtained for the determination of major component safety factors under both rated load and transient breakdown (short circuit) conditions. High speed oscillograph recordings are presented which relate the input current and output current and voltage to the application of short circuits on the output terminals. These oscillograms are also used to determine overcurrent and blink-off time delay ranges.

1. Component Safety Factors for 2KW Rated Load

Oscillograph photographs were taken under full load conditions and component safety factors were determined and recorded in Table II. In cases where transistor collector-to-emitter voltages are higher during start-up or off conditions, the safety factor was determined from the worst condition. Since most of the transistors are operated in the switching mode, dissipation is far below ratings and dissipation safety factors are only determined for the two worst cases.

2. Component Safety Factors with Hydrogen Thyatron and Vacuum Relay Transient Breakdown Devices

Oscilloscope photographs were used to determine the peak component electrical stresses during short circuit applications.

Component safety factors are not redetermined in this section for components which are not significantly affected by the operation of the transient breakdown devices. Test results given in Table III indicate that no component is severely stressed by the operation of the transient breakdown devices. In fact, the results indicate that commutating rectifiers CR45 through CR48 can safely be replaced with rectifiers having a much lower forward current rating. The results indicate that the PIV rating of the output rectifier should be increased from 8,000 volts to at least 11,200 volts to maintain the desired safety factor of 2. This could readily be accomplished. Increasing the safety factors on the power transistors Q1 through Q4 from a minimum of 1.3 to a minimum of 2 cannot be done with presently available transistors. A reduction in input voltage and output load would be required to meet a safety factor of 2 for all conditions. Operation at the present stress

TABLE II. Component Safety Factors with Rated Load

Component	Rating	Electrical Stress	Safety Factor
Transistor Q1 (STC 2118)	I _C Max = 65a V _{CE} Max = 200v Dissipation = 300w.	40a 100v. 18.5w	1.5 2.0 16.2
Transistor Q1 (STC 2118)	I _B Max = 15a V _{EB} O = 10v	7a 3v	2.1 3.3
Transistor Q2 (STC 2118)	I _C Max = 65a V _{CE} Max = 200v	28a 100v	2.3 2.0
Transistor Q2 (STC 2118)	I _B Max = 15a V _{EB} OMax = 10v	6a 3v	2.5 3.3
Rectifier CR4 (Solitron FSPF80W)	PIV = 8000v I _{avg.} = 1.6a	5400v 0.85a	1.5 1.9
Rectifier CR47 (IN 3912)	PIV = 300v I _{avg.} = 35a	100v 0a	3.0 ∞
Rectifier CR48 (IN 3912)	PIV = 300v I _{avg.} = 35a	100v 0.5a	3.0 70.0
Transistor Q19 (2N1016C)	V _{CE} Max = 150v I _C Max = 7.5a	20v(off) 2.6a(on)	7.5 2.9
Transistor Q5 (2N2819)	V _{CE} Max = 80v I _C Max = 25a	20v(off) 2.3a	4.0 10.9
Transistor Q6 (2N2819)	V _{CE} Max = 80v I _C Max = 25a	38v 1.6a	2.1 15.6
Transistor Q12 (2N2102)	V _{CE} Max = 65v I _C Max = 1a	39v 0.3	1.7 3.3
Transistor Q37 (2N1016D)	V _{CE} Max = 200v I _C Max = 7.5a	100v 1.0a	2.0 7.5
Transistor Q11 (2N1016C)	V _{CE} Max = 150v I _C Max = 7.5a Dissipation = 150w	25v(off) 1.4 5w	6.0 5.3 30.0

TABLE III. Component Safety Factors with Hydrogen
Thyratron and Vacuum Relay
Transient Breakdown Devices

Component	Rating	Electrical Stress	Safety Factor
Transistor Q3 (STC 2118)	$I_{CMax} = 65a$ $V_{CEMax} = 200v$	45a 100v	1.4 2.0
Transistor Q3 (STC 2118)	$I_{BMax} = 15a$ $V_{EBO} = 10v$	7a 3v	2.1 3.3
Transistor Q4 (STC 2118)	$I_{CMax} = 65a$ $V_{CEMax} = 200v$	50a 120v	1.3 1.7
Transistor Q4 (STC 2118)	$I_{BMax} = 15a$ $V_{EBO} = 10v$	8.5a 3v	1.8 3.3
Rectifier CR4 (Solitron FSPF80W)	$PIV = 8000v$ $I_{avg.} = 1.6a$	5600v 1a	1.4 1.6
Rectifier CR47 (IN 3912)	$PIV = 300v$ $I_{avg.} = 35a$	110v 0a	2.7 ∞
Rectifier CR48 (IN 3912)	$PIV = 300v$ $I_{avg.} = 35a$	110v <0.5a	2.7 >70.0

level, however, has been very reliable as indicated by the endurance test results.

3. Transient Breakdown Oscillograph Recordings Over Complete Range of Overcurrent and Blink-Off Time Delays

A Century Geophysical Corporation, Model 408, recording oscillograph was used to record input current, output voltage, and output current during short circuit applications. Figure 23 is a calibration oscillogram recorded with full load applied to the power supply.

Figures 24 and 25 show that the maximum and minimum overcurrent time delays are 16 ms and 2 ms, respectively. The maximum and minimum time delays of the blink-off circuit are 96 ms and 2 ms, respectively. These results are within the contract scope of work which states that the overcurrent time delay shall be "two milliseconds (adjustable)" and "after a 2 to 50 milliseconds (adjustable) time delay, the supply shall return soft-on".

Figure 25 shows that the power supply minimum blink-off period actually exceeds 2 milliseconds for two reasons. First, the time constant of the output inductance is equal to the inductance L_2 (3.9 Henry) divided by the winding resistance of the choke ($R_{L2} \approx 50$ ohms at 25°C) and the short circuit path (thyatron or engine arc, wire, and output rectifier). This time constant prevents the output current from decaying below the overcurrent limit in less than seven milliseconds. A second time period is added to the minimum blink-off time delay by an approximate 12 millisecond lag in the starting of the soft-on circuit. (This 12 millisecond time lag can be completely eliminated by selecting a slightly lower voltage Zener diode for Z7.) For these two reasons, the actual minimum blink-off time delay is approximately 19 milliseconds even though the blink-off time delay circuit has the required minimum delay of 2 milliseconds.

It can be seen from Figure 25 that the output current (I_2) does not reach zero during this minimum blink-off period of 19 milliseconds and the hydrogen thyatron breakdown device remains in conduction. The power converter therefore increases the output current in a soft-on fashion at the end of each blink-off period in accordance with the contract scope of work. Figure 26 shows the output voltage transient when the short circuit was removed by a vacuum relay. The energy from the output filter choke (L_2) rapidly charges the output capacitor (C_2) to a safe peak level of 1400 volts before the soft-on cycle commences. This result indicates that the design of the output filter is more than adequate to protect the converter semiconductors from peak voltages during short circuit removal.

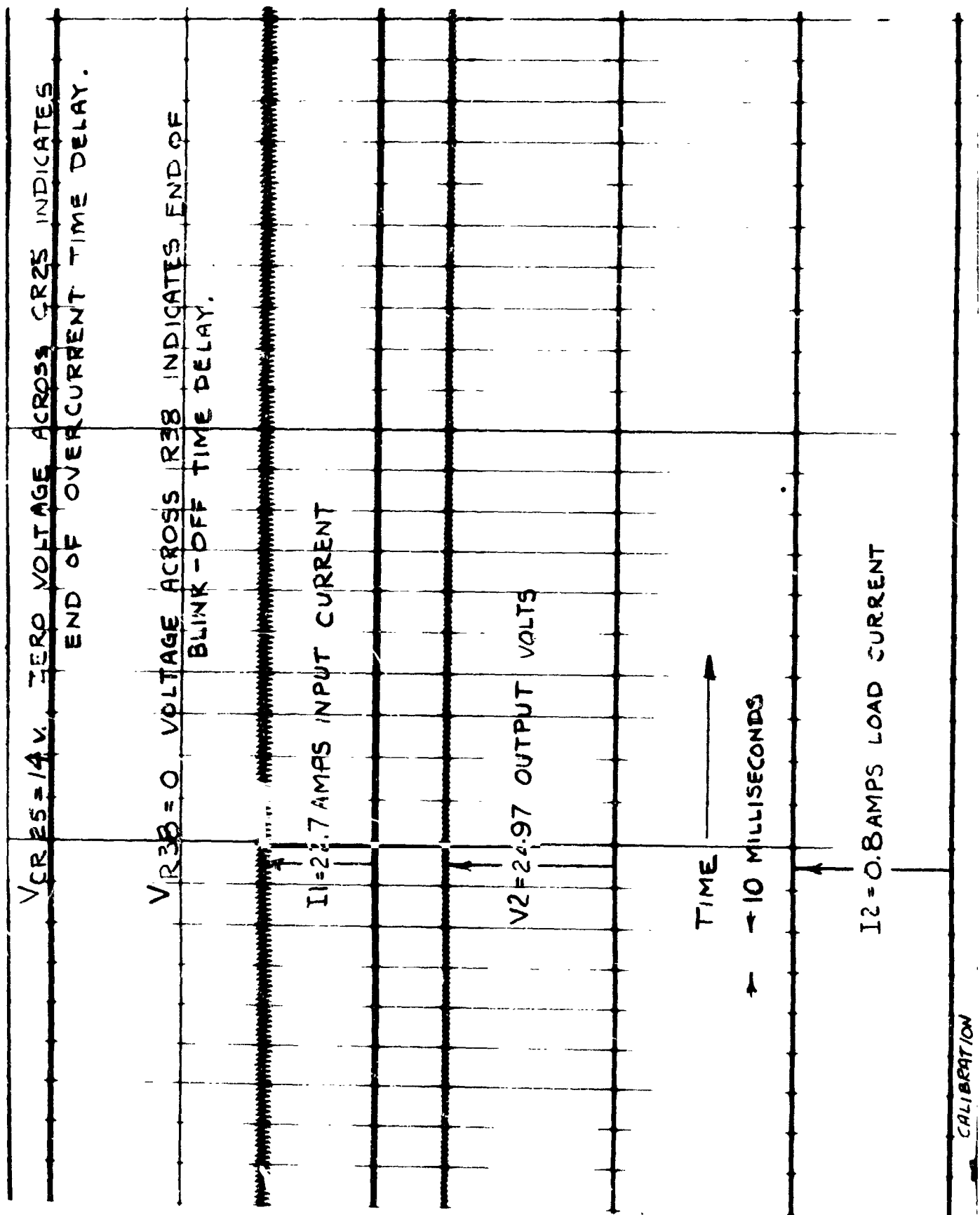


FIGURE 23. Calibration Oscillogram Showing Normal Full-Load Operation

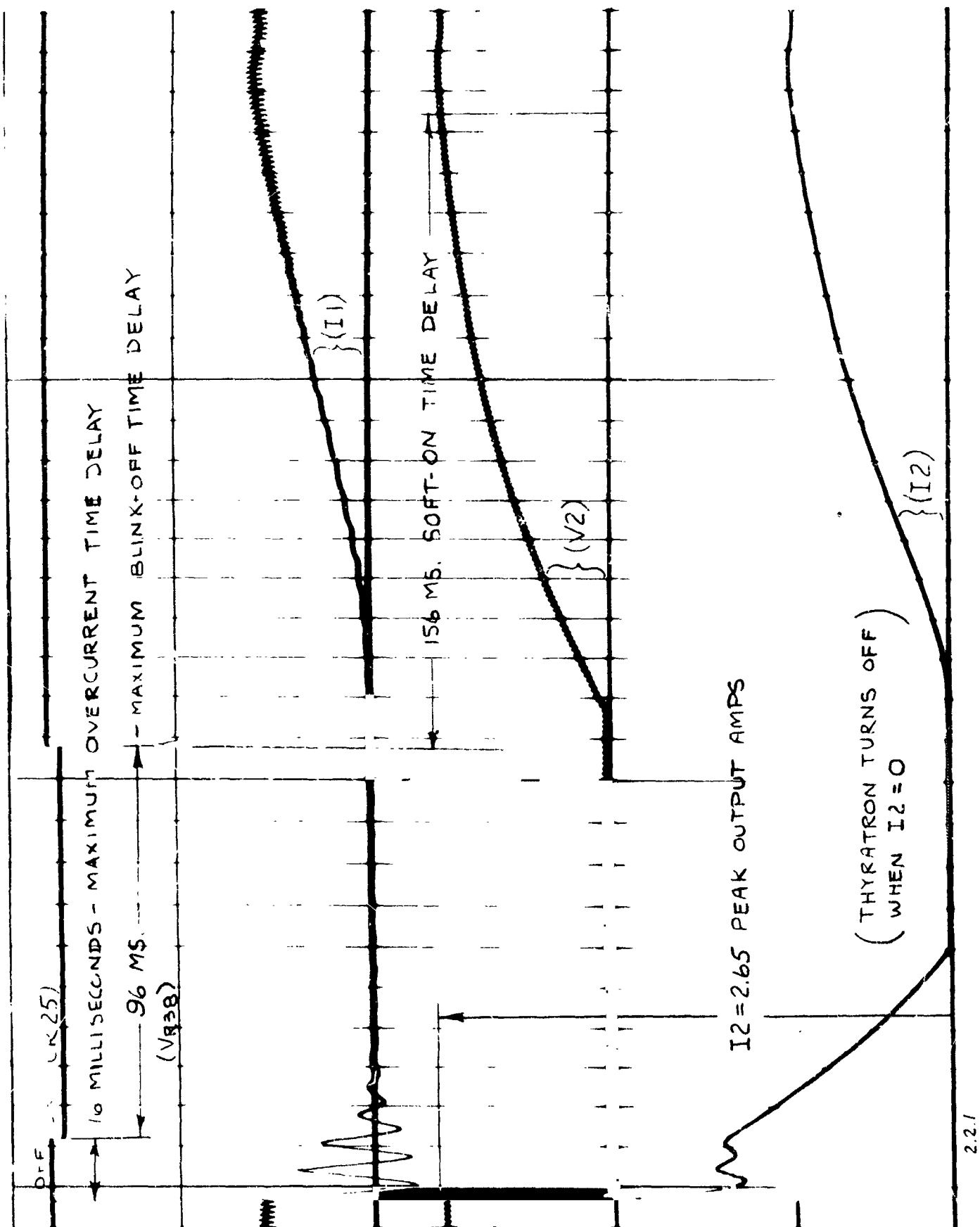


FIGURE 24. Oscillogram Showing Application of Short Circuit with Maximum Overcurrent and Blink-Off Time Delays

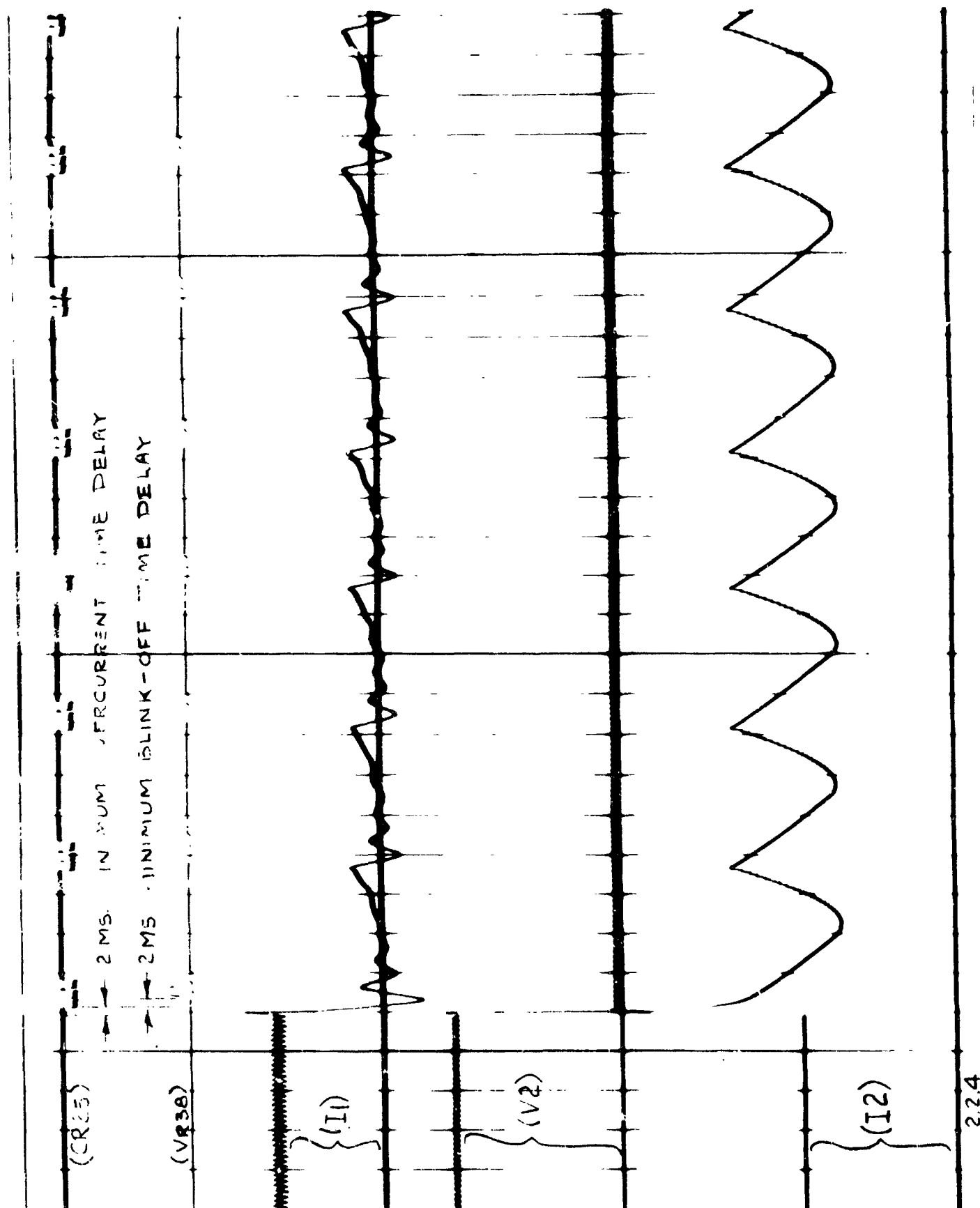


FIGURE 25. Oscilloscope Showing Application of Short Circuit with Minimum Overcurrent and Blink-Off Time Delays

WAED65. 12E-44

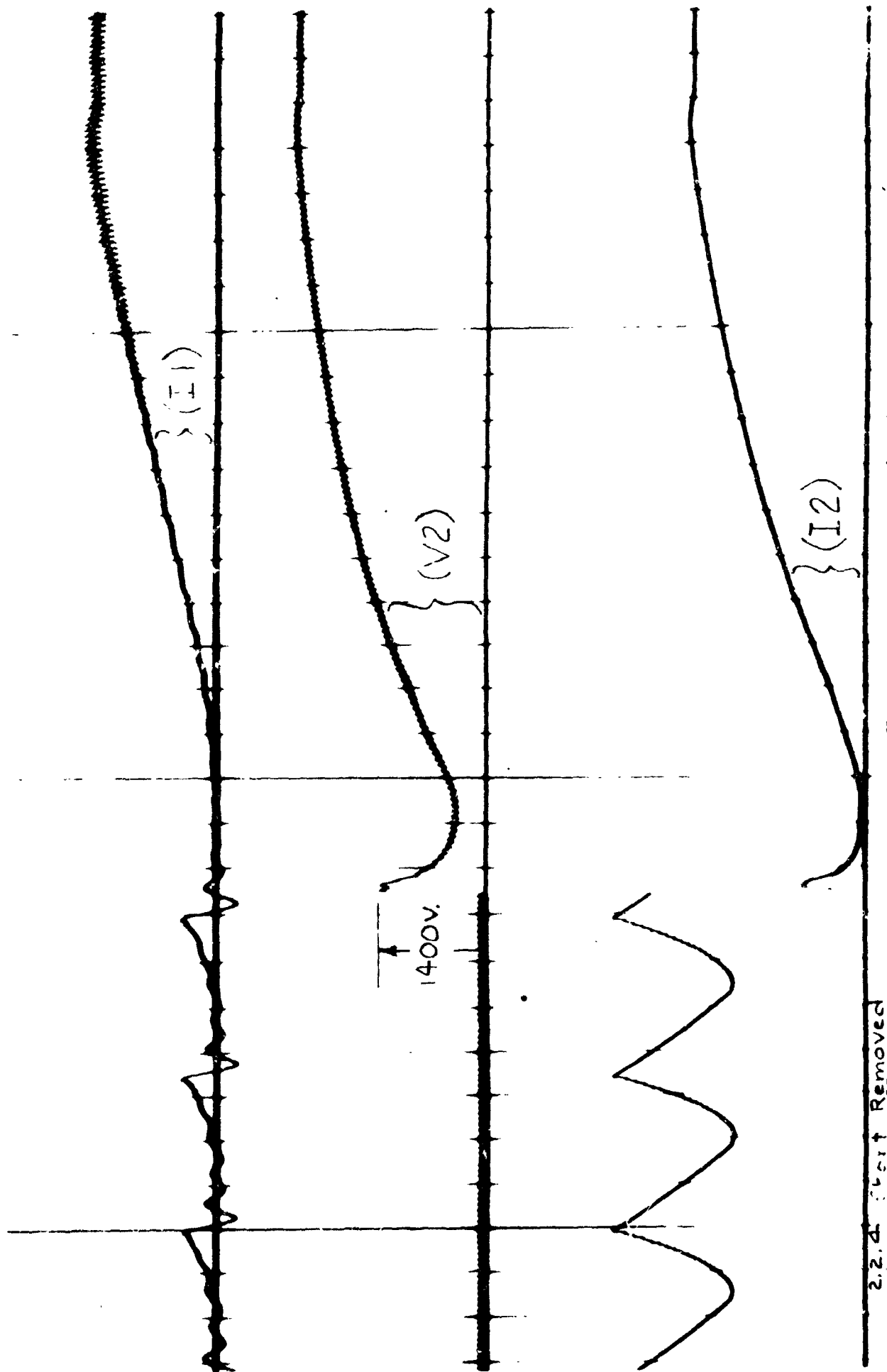


FIGURE 26. Oscillogram Showing Removal of Short Circuit with Vacuum Relay

WAED65.12E-45

Figure 27 shows the application of a short circuit to the power converter with a vacuum relay. There is some indication of contact bounce but the peak output current appears to be about the same as with short circuits applied by the hydrogen thyatron. This peak current (2.65 amps) is primarily determined by resistors R90 through R97 (a total resistance of 1020 ohms) which were first added to the Breadboard Model limit the peak discharging current from the output capacitors (C2) to 2.5 amperes and thereby prevent damage of the overcurrent sensing circuit.

Figure 28 shows that the power converter output can be interrupted by a low level control signal in accordance with the contract scope of work. The low level control signal, used to initiate the power interruption, was the grounding of the base of transistor Q23 with switch SW1. This could also be accomplished, if desired, by turning on transistor Q24 with 0.1 milliampere base current. Either of these procedures initiates the overcurrent time delay and causes the power converter to blink-off and remain off until the low level signal is removed. Then the power converter will automatically return soft-on.

The oscillogram of Figure 29 demonstrates that the power converter can withstand the short time application of a short circuit without the necessity of turning off the power converter. Such a short circuit may occur in practice if an ion thruster arcs and burns clear in less time than the overcurrent time delay (2 to 16 milliseconds). In this case, the power converter supplies current to the fault at a safe magnitude of 1.15 amperes and returns very rapidly to rated output voltage when the fault is removed. It was physically impossible to simulate this type of fault with a vacuum relay because the relay could not be made to close and open in less time than the overcurrent time delay. Therefore it was necessary to disable the blink-off circuit during this test by connecting together the anode and cathode of CR25. Figure 29 shows that the power converter safely returns to normal full load operation after the removal of the short circuit as required by the contract scope of work.

D. ENDURANCE TESTS

It is required by the contract scope of work that the power supply demonstrate "a minimum of 10 hours of operation with a dummy load having transient load-inducing capability The supply shall not be damaged by any of these transients, nor shall any performance deterioration occur". This requirement was met by operating the power converter continuously for seven hours with full load applied and six hours with a transient type load applied. The temperature rise of major components was recorded during these endurance tests.

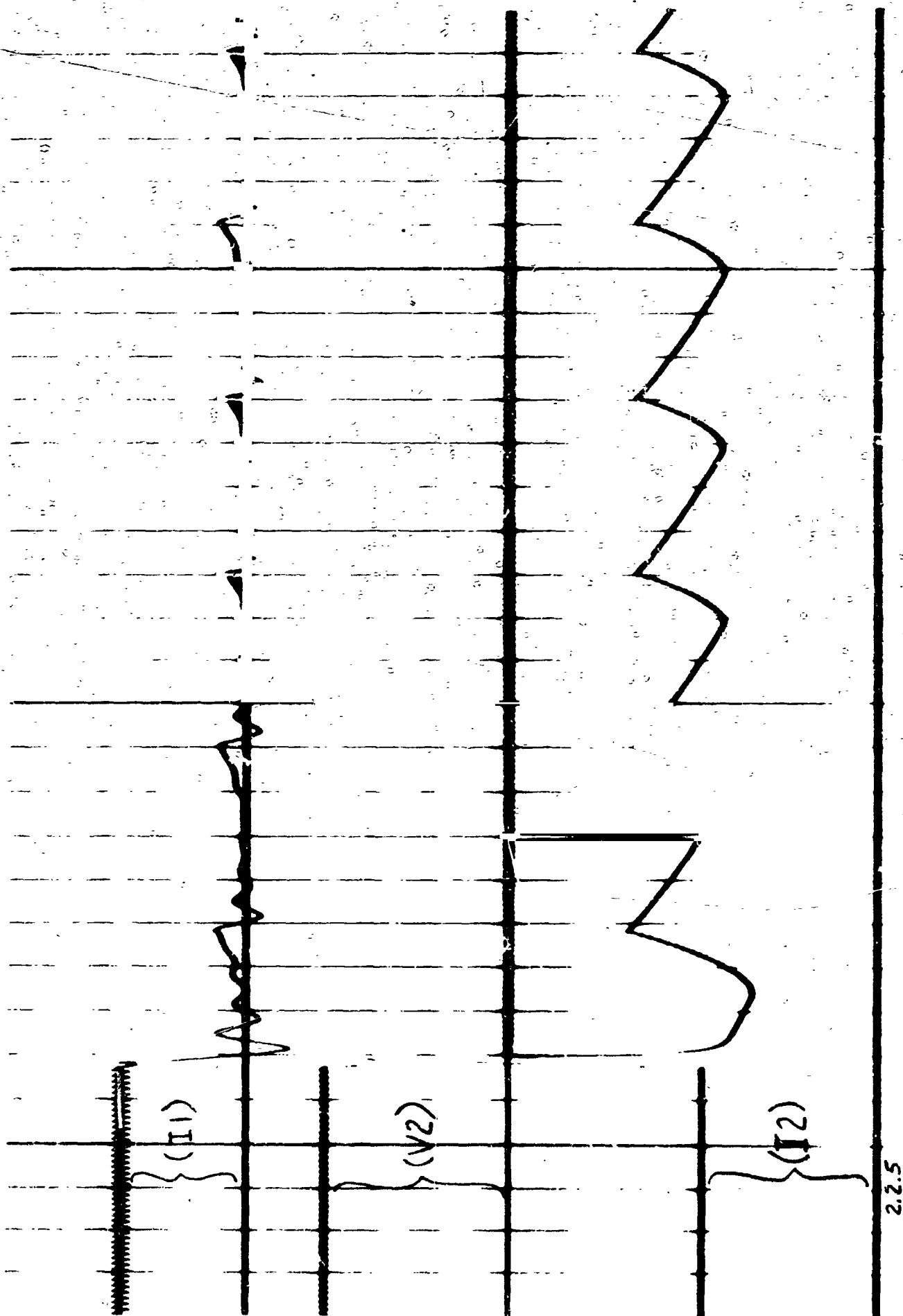


FIGURE 27. Oscillogram Showing Application of Short Circuit with a Vacuum Relay

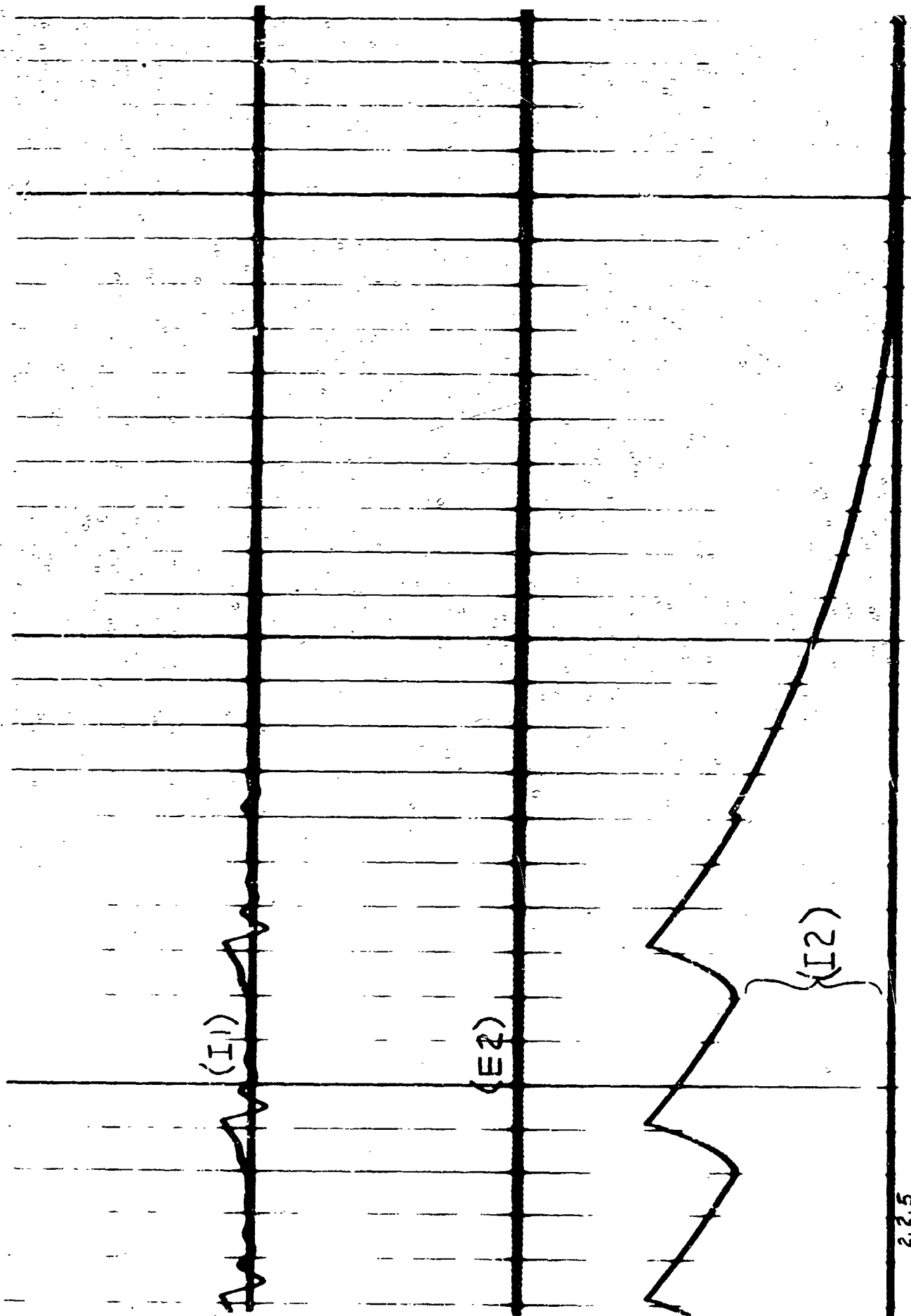


FIGURE 28. Oscilloscope Showing Shut-Down of Power Converter with Low Level Control Signal

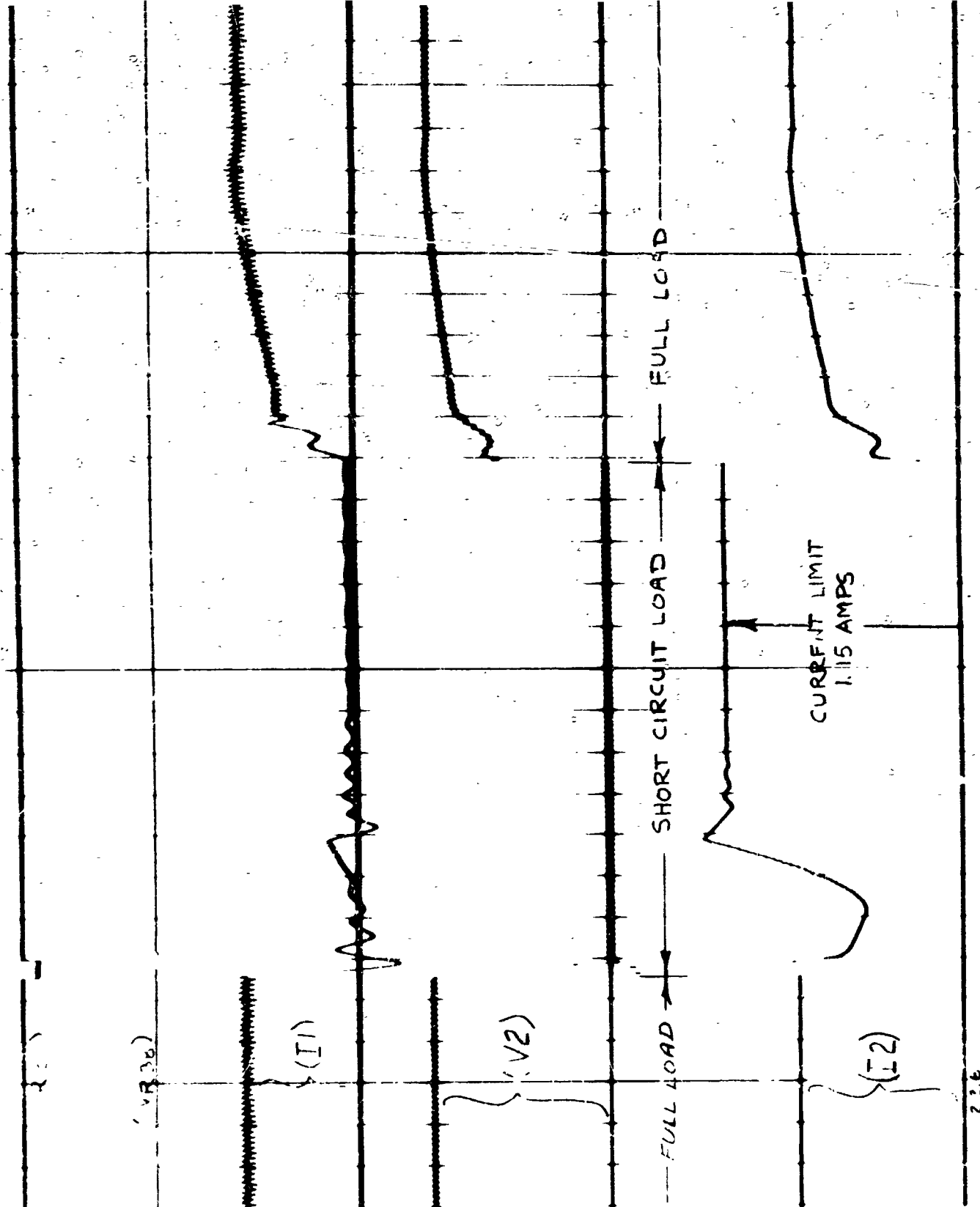


FIGURE 29. Oscillogram Showing Application and Removal of Short Circuit

The 6-hour transient load endurance test caused a lower component temperature rise than the full load endurance test. The transient load consisted of one minute of 2KW load and one minute of short circuit. This cycle was repeated for 6 hours which caused 360 short circuit transients. During each minute of short circuit operation, the power converter blinked-off and came soft-on approximately ten times per second for a total of approximately 108,000 blink-off and soft-on cycles.

The maximum temperature reached by any component was 142°C for the output transformer, T1. This maximum temperature was reached during the full load test and is well below the safe operating temperature of 250°C for this transformer.

There was no component failure or performance deterioration which occurred during any of the 13 hours of the endurance test or during the performance of any of the tests required by this contract.

VI. WEIGHT, LOSS, AND PERFORMANCE CONSIDERATIONS

The weight of all electrical components in the Experimental Model (excluding meters, switches, and receptacles) is 28.19 pounds. The component types are listed in Table IV according to descending weight. This table also lists the weight of each item as a percentage of total weight. From this weight analysis, it is obvious which items should be considered to accomplish major weight reductions.

Without changing the performance requirements of this power supply, the electrical stress tests have shown that significant component rating reductions can be made on components listed on lines 3, 9, 10 and 12. The weight of these components, representing 9.7% of the total weight, could be cut in half without affecting performance. However, the preceding test results also indicate that the capacitance of the input filter capacitor, C1, should be increased to meet the input ripple performance requirements, and the output rectifier voltage rating should be increased 50% to meet the required safety factor of 2. These two changes would increase the total component weight by approximately 1.5%.

The maximum efficiency of the power converter with 2KW resistive load is 87.86%. This represents a power loss in the converter of 276 watts. The sources of this loss are given in Table V.

With the performance requirements of this contract, Tables IV and V indicate that very little more can be done to improve efficiency and reduce weight. However, these tables indicate clearly which performance requirements have the largest effect on weight and efficiency. It is apparent that the input and output filter components offer the greatest opportunity to improve weight and efficiency. For example, elimination of the 2% rms and 5% peak limits on input current ripple would allow L1 and C1 to be eliminated and save 1.57 pounds (5.57% of all component weight) and 5 watts (1.81% of all component losses).

The maximum improvement in weight and efficiency could be accomplished by eliminating the overcurrent time delay and current limiting requirements. This performance change would allow the output choke to be reduced by approximately 10 pounds (35.47% of all component weight) and 40 watts (14.5% of all component losses).

With these two changes in performance requirements, it should be possible to build the power converter, operating at 800 cps, with a total component weight of 14.3 pounds and an efficiency of 89.5%. By approximately doubling the operating frequency, the power transistor switching losses would be increased approximately 50 watts but the output transformer and other magnetic component weights could be decreased by an additional estimated total of 3

TABLE IV. Component Weight Analysis

	Item	Component Description	Qty.	Weight/Item (lbs)	Total Weight of Component Type (lbs.)	% of All Component Weight	Weight Subtotals (lbs)	Percentage Sub-totals
1	L2	Output Choke 3.2H.	1	12.10	12.10	42.9	12.10	42.9
2	T1	Output Transformer	1	8.00	8.00	28.4	20.10	71.3
3	C2	Output Filter Capacitor	3	0.65	1.95	6.9	22.05	78.2
4	L1	Input Choke .208 mh.	1	0.89	0.89	3.2	22.94	81.4
5	Q1,2,3,4	Power Transistor 2SC2118	4	0.21	0.84	3.0	23.78	84.4
6	T2,3,4,5	Base Drive Transformer	4	0.20	0.80	2.8	24.58	87.2
7	C1	Input Filter Capacitor	47	0.0144	0.68	2.4	25.26	89.6
8	L3	Power Supply Choke 40 mh	1	0.44	0.44	1.6	25.70	91.2
9	Q5-10	Drive Transistors 2N2891	6	0.066	0.39	1.4	26.09	92.6
10	CR45-48	Commutating Rectifier IN3912	4	0.05	0.20	0.7	26.29	93.3
11	CR1,2,3,4	High Voltage Rectifier	1	0.20	0.20	0.7	26.49	94.0
12	CR7,8,16,17,18,50,52,54,56	Rectifier IN3890 (100V - 12 amp)	9	0.019	0.17	0.6	26.66	94.6
13	All others	Small resistors, diodes, transistors, capacitors.	210	0.0073 average	1.53	5.4	28.19	100.0

TABLE V. Component Loss Analysis

Line	Item	Component or Circuit Description	Qty.	Loss/Item or Circuit (watts)	Total Loss of Component or Circuits(watts)	% of All Component Losses
1	Q1,2,3,6	Power Transistor STC2118	4	22	88	31.88
2	L2	Output Choke 3.9H	1	52	52	18.84
3	T1	Output Transformer	1	48	48	17.39
4	R1,2,31, 32;CR49- 56;T2-5	Current Feedback Base Drive Circuits	16 (4 cir- cuits)	6 per circuit	24	8.70
5	Q11,32, 33,37; T12;L3; R17-20,22; CR16;C7,15; Z5,13.	DC Chopper and Regulator Circuit	16 (1 cir- cuit)	14	14	5.07
6	CR1-4	High voltage Recti- fier	1	13	13	4.71
7	R77-79	High Voltage Resistance	3	4	12	4.35
8	L1	Input Choke	1	5	5	1.81
9	All Others	Control Circuits and miscellaneous other components	249	0.008 average	20	7.25

pounds. With the two changes in performance requirements and the increase in operating frequency, it should be possible to build the 2KW power converter with a total component weight of 11.3 pounds and an efficiency of approximately 85%.

VII. CONCLUSIONS AND RECOMMENDATIONS

The evaluation of the Breadboard and Experimental Models has been successful and the contract performance requirements have been met in all important respects. The purpose and goals of Phase I of the contract have been met.

The specific approach of using a pulse width modulated bridge inverter with silicon power transistors and current feedback base drive has been proven to be a feasible and desirable method of building a reliable, efficient, and lightweight power converter for ion thrusters.

The use of a pulse width modulated bridge inverter in conjunction with a soft-on starting sequence eliminates any possibility of saturating the output transformer during start-up transients. This method always applies a very narrow pulse width to the output transformer during the beginning of each soft-on cycle. This is an advantage over the two-transformer phase-shift regulation method where full-width square wave voltages are applied to both output transformers under all operating conditions.

Some component failures occurred during the preliminary check out of the Experimental Model. These failures were the result of wiring errors, testing errors, and a defective component and were not caused by a design deficiency or low safety factor. After the preliminary check out, no component failures occurred during the entire test program which included over 400 short circuit applications and over 100,000 blink-off and soft-on cycles. These results are an indication of high reliability. However, the final determination of reliability must be made with the power supply operating an ion thruster.

The component electrical stress tests indicated that most semiconductor component safety factors were above the design objective of two. Some components, like the base drive and pulse transistors, have excessively high safety factors. This resulted from resistors R68-75 being added to reduce peak transistor currents during the Breadboard Model development. In the future, transistors Q5 through Q10 should be replaced with transistors having much lower collector current ratings. The average current ratings of rectifiers CR7, 8, 17, and 18 and commutating rectifiers CR45 through CR48 should also be significantly reduced.

The lowest measured safety factor was 1.3 for the current rating of an output transistor. Since no 200 volt transistors are currently available with current ratings above 65 amperes, no component changes are now possible to increase this safety factor.

Output transformer voltage transients (ringing) caused the present output rectifier safety factor to be as low as 1.4. It is recommended that the most

efficient solution to this problem is to increase the voltage rating of the output rectifier by 50%. A sizeable reduction in ringing voltage would be possible if the overcurrent time delay and current limiting requirements were eliminated so that the size of the output choke could be greatly reduced.

The weight and loss analyses of Section VI indicate that the electrical component weight could be reduced from 28.19 pounds to approximately 11.3 pounds at 85% efficiency if two performance requirements were eliminated. These are the input current ripple requirement of 5% maximum and the overcurrent time delay with current limiting. With the latter change, the inverter would be made to blink-off immediately upon application of an overcurrent condition. This would eliminate the need for a large output choke to limit the increase in transistor current during the response time of the pulse-width-modulation type current limiting circuit. Some output filter would still be required to meet the output voltage ripple requirements. The energy from this filter would still be transferred to an overcurrent fault. After the blink-off time delay or after the output current went below the overcurrent limit, whichever occurred first, the converter would automatically return soft-on. An indication of how this change would affect ion thruster operation could be obtained by setting the overcurrent time delay to zero in the Experimental Model by disconnecting capacitor C10.

It is recommended that these performance changes be considered for Phase II of this program so that the associated weight reductions could be verified in radiation cooled power supply modules.

APPENDIX A.

PARTS LIST FOR EXPERIMENTAL MODEL

<u>ITEM¹</u>	<u>DESCRIPTION</u>
AR1	Transductor
AR2, 3	Saturable Reactor
AR4	Saturable Reactor
C1	Capacitor, 1222 μ F, 200V
C2	Capacitor, 0.25 μ F, 5000 V
C3, 15	Capacitor, 40 μ F, 30 VDC
C7	Capacitor, 36 μ F, 100 VDC
C8, 10, 12A	Capacitor, 1 μ F, 150 V
C9	Capacitor, 0.56 μ F, 200 V
C11	Capacitor, 2 μ F, 100 VDC
C12	Capacitor, 22 μ F, 35 VDC
C13	Capacitor, 150 μ F, 40 VDC
C14	Capacitor, 0.22 μ F, 100 V
C15	Capacitor, 0.01 μ F, 150 V
C17	Capacitor, 0.0068 μ F, 600 V
CR1, 2, 3, 4	Rectifier, 8000 V 1.6 Amp Bridge
CR5, 6, 9, 10, 11, 12, 19, 20, 31, 32, 33, 36, 37, 38, 39, 59, 60, 61, 62, 63, 64, 65	Diode, 1N914
CR7, 8, 16, 17, 18, 50, 54, 54, 56	Diode 1N3890
CR21, 22, 23, 24, 26, 27, 28, 29, 30, 34, 35, 40, 41, 42, 66	Diode, 1N645
CR25	Rectifier, Silicon Controlled, 2N2324A
CR43, 44, 49, 51, 53, 55, 58	Diode, UTR12
CR45, 46, 47, 48	Diode, 1N3912
J1	Receptacle, MS 3102A-20-24P
J2	Receptacle, 560/U

(1) For item locations see Schematic Diagram, Figure 2.

<u>ITEM</u>	<u>DESCRIPTION</u>
L1	Reactor, 0.208 mH
L2	Reactor, 3.9 H
L3	Reactor, 40 mH
M1	Voltmeter, 0-150 volts DC
M2	Voltmeter, 0-3000 volts DC
Q1, 2, 3, 4	Transistor, Power, STC 2118
Q5, 6, 7, 8, 9, 10	Transistor, 2N2819
Q11, 19	Transistor, 2N1016C
Q12, 13, 14, 15, 16, 17, 18, 21, 22, 23, 24, 26, 28, 31, 32, 33, 34, 35, 36	Transistor, 2N2102
Q20	Transistor, Unijunction, MM/2N491B
Q25, 27	Transistor, 2N2905
Q29, 30	Transistor, 2N2034
Q37	Transistor, 2N1016D
R1, 2, 7, 8, 31, 32	Resistor, 100 ohms, 1W, CC
R3, 6	Resistor, 270 ohms, 2W, CC
R4, 5	Resistor, 200 ohms, 2W, CC
R9, 10, 11, 12	Resistor, 27 ohms, 1W, CC
R13, 14	Resistor, 1200 ohms, 5W, WW
R15, 16	Resistor, 680 ohms, 1/2W, CC
R17	Resistor, 3K ohms, 10W, WW
R18	Resistor, 6 ohms, 2W, WW
R19, 20, 26, 29, 30, 42, 44, 49, 86, 87, 99	Resistor, 10K ohms, 1/2W, CC
R21	Resistor, 4.7K ohms, 1/2W, CC
R22, 81	Resistor, 75 ohms, 2W, WW
R23	Resistor, 3.9K ohms, 1/2W, CC
R24	Resistor, 82 ohms, 1W, CC
R25	Resistor, 390 ohms, 1/2W, CC
R27, 28, 52, 59, 64, 80, 98	Resistor, 2K ohms, 1/2W, CC
R33	Resistor, 33K ohms, 1/2W, CC
R34, 48	Resistor, 51K ohms, 1/2W, CC
R35, 43, 47, 85	Resistor, 20K ohms, 1/2W, CC
R36, 40, 46	Resistor, 2K ohms, 2W, WW
R37, 65, 66, 88	Resistor, 470 ohms, 1/2W, CC
R38	Resistor, 47 ohms, 1/2W, CC
R39, 55	Resistor, Variable, 100K ohms, 3W
R41, 53	Resistor, 270 ohms, 1/2W, CC
R45	Resistor, Variable, 20K ohms, 3W
R50, 63, 89	Resistor, 150 ohms, 1/2W, CC
R51, 56, 67, 82, 83, 84	Resistor, 1K ohms, 1/2W, CC
R53	Resistor, 50 ohms, 5W, WW

<u>ITEM</u>	<u>DESCRIPTION</u>
R57	Resistor, Variable, 100K ohms, 2W, WW
R58	Resistor, 68K ohms, 1/2W, CC
R60	Resistor, Variable, 2K ohms, 1.5W, WW
R61	Resistor, Variable, 500 ohms, 2W, WW
R62	Resistor, 1K ohms, 2W, WW
R68, 69, 70, 71, 72, 73, 74, 75	Resistor, 15 ohms, 2W, CC
R76	Resistor, 200 ohms, 5W, WW
R77, 78, 79	Resistor, 180K ohms, 15W, WW
R90, 91, 92, 93, 94, 95, 96,	Resistor, 510 ohms, 1W, CC
SW1, SW2	Switch, Toggle, SPDT
T1	Transformer, Power,
T2, 3, 4, 5	Transformer, Base Drive
T6, 7, 8	Transformer, Pulse Turn-off
T9	Transformer, Oscillator
T10	Transformer, Slave Oscillator
T11	Transformer, Drive Oscillator
T12	Transformer, Chopper Drive
Z5	Diode, Zener, 10W 20-22V
Z6	Diode, Zener, 400MW 10V
Z7	Diode, Zener, 10W 8.2V
Z8, 9, 10, 12, 17	Diode, Zener, 400MW 8.2V
Z11	Diode, Zener, 400MW 12V
Z13	Diode, Zener, 1W 15V
Z18, 19	Diode, Zener, 10W 12V